AD-A191 044 EXPERIMENTAL INVESTIGATION OF A THREE-STAGE RAILGUN INCORPORATING PUFF-SW..(U) MATERIALS RESEARCH LABS ASCOT VALE (AUSTRALIA) D R SADEDIN ET AL. MAY 87 1/1

UNCLASSIFIED MRL-R-1056 DODA-AR-005-135 F/G 20/3 NL

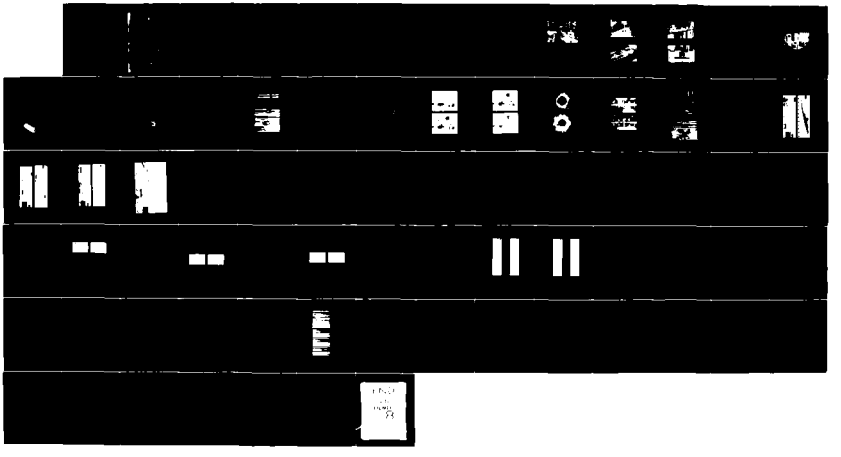

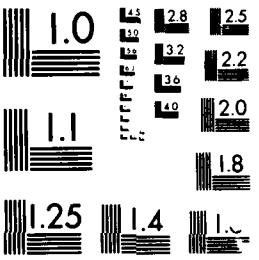

MICROCOPY RESOLUTION TEST CHART
NATIONAL BUREAU OF STANDARDS 1963-A

(4)

MRL-R-1056

AR-005-135

DEPARTMENT OF DEFENCE

DEFENCE SCIENCE AND TECHNOLOGY ORGANISATION

MATERIALS RESEARCH LABORATORIES

MELBOURNE, VICTORIA

REPORT

MRL-R-1056

EXPERIMENTAL INVESTIGATION OF A THREE-STAGE RAILGUN INCORPORATING PUFF-SWITCHING

D.R. Sadedin and D.F. Stainsby

Approved for Public Release

DSTO MRL MARIBYRNONG

DEPARTMENT OF DEFENCE
MATERIALS RESEARCH LABORATORIES

REPORT

MRL-R-1056

EXPERIMENTAL INVESTIGATION OF A THREE-STAGE RAILGUN INCORPORATING PUFF-SWITCHING

D.R. Sadedin and D.F. Stainsby

ABSTRACT

A sequence of four firings of a 2.4 m long, 10 mm square bore railgun is described and analysed. The railgun comprised an injection stage, a breech power source and a second power source which was connected by a "puff-switch". The report deals with the puff-switching results, distribution of current in the plasma, the proportion of projectile kinetic energy due to plasma expansion forces as compared to electromagnetic forces, the correlation of rail damage with current and plasma length, and velocity limitation according to the ablation model.

POSTAL ADDRESS: Director, Materials Research Laboratories
P.O. Box 50, Ascot Vale, Victoria 3032, Australia

CONTENTS

SECURITY CLASSIFICATION OF THIS PAGE **UNCLASSIFIED**

DOCUMENT CONTROL DATA SHEET

REPORT NO.	AR NO.	REPORT SECURITY CLASSIFICATION
MRL-R-1056	AR-005-135	Unclassified

TITLE

Experimental investigation of a three-stage railgun incorporating puff-switching

AUTHOR(S)
D.R. Sadedin and
D.F. Stainsby

CORPORATE AUTHOR
Materials Research Laboratories
PO Box 50,
Ascot Vale, Victoria 3032

REPORT DATE	TASK NO.	SPONSOR
May 1987	DST 82/212	DSTO

FILE NO.	REFERENCES	PAGES
G6/4/8-3213	15	XX

CLASSIFICATION/LIMITATION REVIEW DATE	CLASSIFICATION/RELEASE AUTHORITY
February 1990	Superintendent, MRL Physics Division

SECONDARY DISTRIBUTION

Approved for Public Release

ANNOUNCEMENT

Announcement of this report is unlimited.

KEYWORDS

Railgun accelerators
Electromagnetic launchers
Distributed energy railgun
Plasma switching

SUBJECT GROUPS 0081B 0046G 0079G

ABSTRACT

A sequence of four firings of a 2.4 m long, 10 mm square bore railgun is described and analysed. The railgun comprised an injection stage, a breech power source and a second power source which was connected by a "puff-switch". The report deals with the puff-switching results, distribution of current in the plasma, the proportion of projectile kinetic energy due to plasma expansion forces as compared to electromagnetic forces, the correlation of rail damage with current and plasma length, and velocity limitation according to the ablation model.

EXPERIMENTAL INVESTIGATION OF A THREE-STAGE RAILGUN INCORPORATING PUFF-SWITCHING

1. INTRODUCTION

Practical railguns will almost certainly have several propulsive stages. Firstly, it is highly desirable that the projectile enter the actual railgun at a velocity of at least 1 km/s. This lessens the rail damage which the plasma arc in the railgun causes if it is required to accelerate the projectile from rest. Secondly, it is desirable to supply power at points along the rails instead of using one large power source at the breech. This reduces the energy that is lost both in resistance and in stored magnetic energy of the rails when only a breech supply is used. Efficiency is therefore enhanced.

In this report the results are given of test firings of a railgun comprising a powder gun for the first stage and two electrical stages.

The work reported here was carried out early in 1986 and was the final phase of the MRL railgun program. The work which culminated in this phase is reported in Reference 9.

1.1 Puff Switching

In 1979 and 1980 Marshall [1,2] investigated the possibility of directly connecting power supplies at points along the rails as shown in Fig. 1. He calculated efficiencies in the range 70 to 90% on the assumption that rail resistance and stored magnetic energy losses were the only railgun losses. He called this the Distributed Energy Store (DES) scheme. Parker [3] and Holland [4,5] and Tower and Haight [6] have also reported upon it. Not all losses are reduced by the DES scheme. The plasma arc loss, for example, is not reduced. The above efficiencies are therefore maximum attainable values.

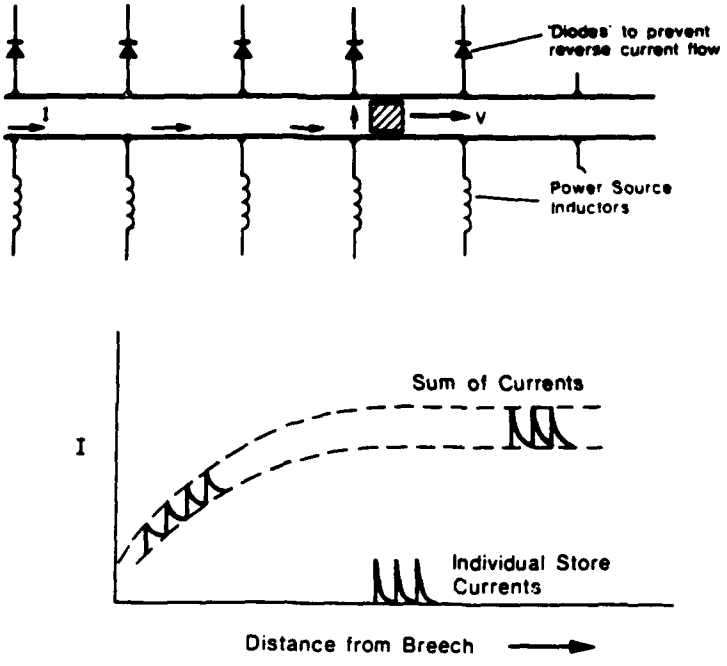

FIG. 1 Distributed energy source scheme

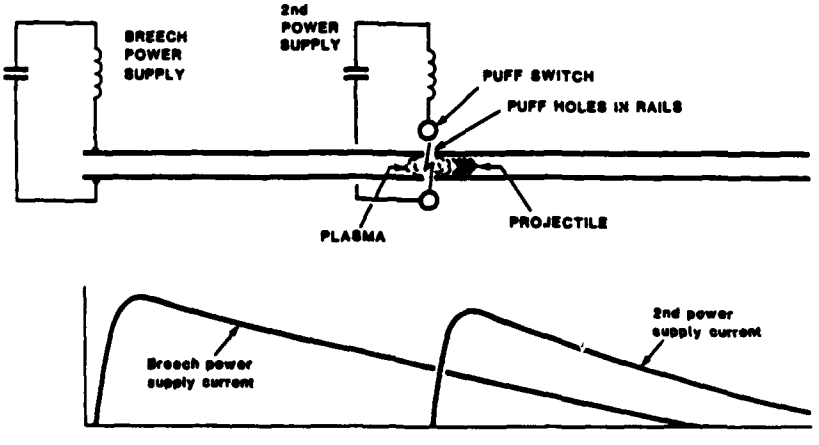

FIG. 2 Puff-switching concept

The scheme requires means for sensing when the projectile has reached the point where an energy store is to be connected and also for making the connection. Marshall [7] suggested that in plasma armature guns some of the ionized plasma be allowed to escape through holes in the rails and used to trigger an arc-switch between the rails and the power source, as in Fig. 2. He called the holes "puff-holes" and the technique "puff-switching".

The railgun used in the experiments reported here incorporated a single "puff-switch" to test this concept.

2. THE EXPERIMENTS

2.1 General Description

A 2.4 m long railgun with two electrical power stages and a powder gun injector was used. The system is shown in Fig. 3. One power source was connected at the breech end and the other was connected by a puff-switch through puff-holes at a point 900 mm further along the rails.

In concept, when the projectile passed this point, some of the high pressure plasma could pass through the puff-holes in the rails and initiate breakdown between the puff-switch electrodes and the rails, thereby connecting the second power source to the railgun.

The 900 mm position was selected as a point where the breech power source current would have fallen sufficiently for the current from the second power source to cause a sudden increase in plasma velocity. However the breech supply current must not have fallen so much that the plasma pressure would be insufficient to operate the puff-switch.

A sequence of four firings is reported here. The first was performed without electrical power, i.e. only the injector stage was fired, coupled to the railgun. This was done to determine the effects of the injector gases and of drag and air load in the railgun bore. Another firing used only the injector and the breech power supply and its purpose was to provide a reference for comparison with the puff switching shots. Two further shots were conducted with all three stages, i.e. the injector, the breech and puff-switched power supplies, operative.

FIG. 3 General view of 2.4 m railgun system

(a)	railgun,	(e)	mirror
(b)	puff switch vents	(f)	camera
(c)	capacitors	(g)	flash screen
(d)	inductor	(h)	catch tank

2.2 Equipment and Operation

The 2.4 m long railgun is shown in Figs. 4-7. It had a 10 mm square bore and cadmium copper rails 16 mm x 5 mm in cross section. The rails were rubbed to a smooth finish on the bore sides with emery paper to remove any surface burrs and nicks. They were mounted in a two-piece body made of clear polycarbonate which was bolted together at 50 mm intervals. Rail edges were bevelled and the corners in the rail channels in the body were rounded to reduce corner stresses and the development of cracks in the body. The clear body enabled streak photography to be used to record the plasma position with the aid of a marker bar assembly which was laid on top of the body.

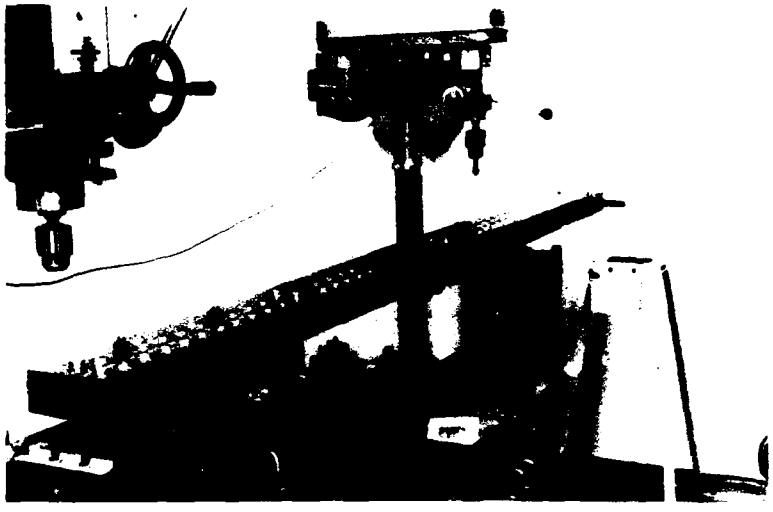

FIG. 4 Machining holes in body of 2.4 m railgun for puff-switch electrodes

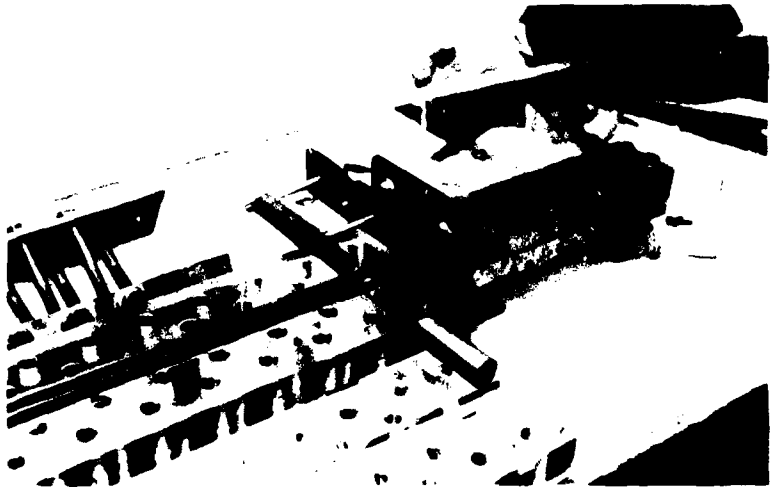

FIG. 5 Breech end of 2.4 m railgun showing current connection electrodes and injector body

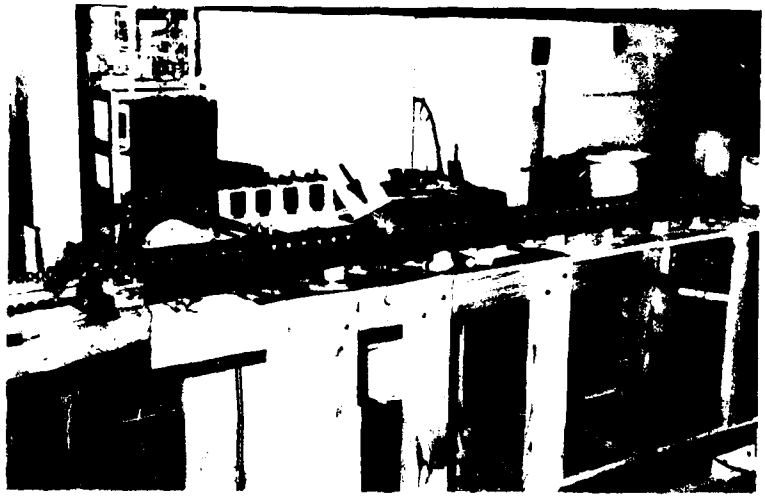

FIG. 6 2.4 m railgun mounted on firing bench. Puff-switch electrodes are visible (arrow)

FIG. 7 View of puff-switch electrode region and marker bars. The distance between marker bars was 100 mm.

Optimum puff-hole size was not easily determinable prior to the experiments. In the first puff-switching experiment 2 mm diameter holes were used whilst in the second they were reduced to 0.38 mm diameter.

Ten magnetic pick-up coils were inserted into the polycarbonate body beneath the rails, as shown in Fig. 8, to record the magnetic effects of the plasma.

The breech power source, Figs. 9 and 12, was made up of a 4,000 μF capacitor bank (20 capacitors, Maxwell type 3378, 200 μF, 10 kV) and a 6.3 μH inductor. The capacitor bank was switched into the railgun circuit by an ignitron approximately 78 μs after a fibre optic probe in the injector detected the flash from the burning powder. The 78 μs delay was used to enable the projectile to move a few centimetres past the rail current-connection-points before the current was applied to the armature. A spark gap, triggered upon sensing voltage reversal across the capacitors, was used to convert the breech drive to inductive - only after peak current [8].

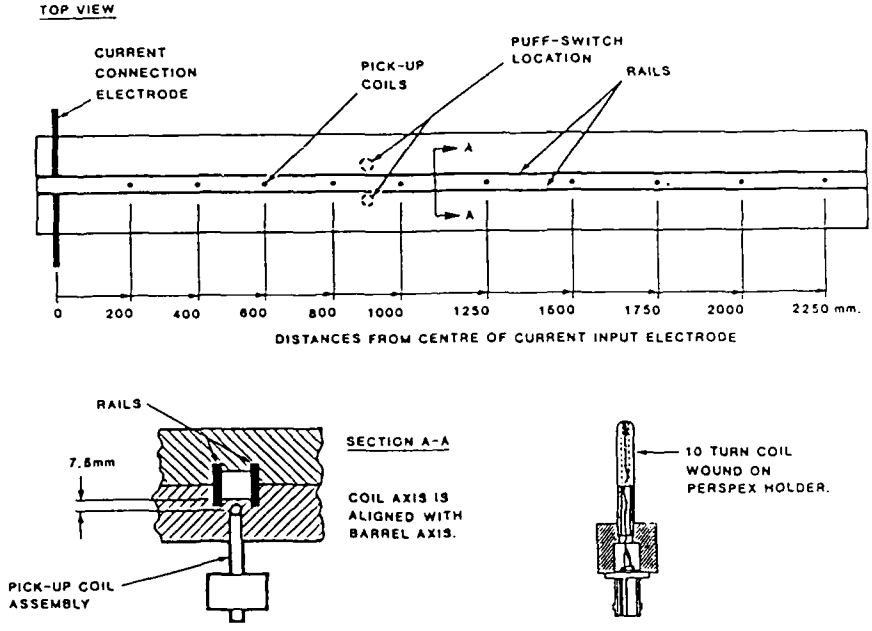

FIG. 8 Pick-up coils and location on 2.4 m railgun

Injection velocity was determined using the signals from the first flash detector and a second detector located in the railgun body at a distance of 40 mm from the first flash detector.

The puff-switched power supply, Fig. 12, consisted of a 2000 μF capacitor bank, a 6.3 μH inductor and a diode-triggered spark gap crowbar switch. It did not have an ignitron because the puff-switch performed the connection function.

FIG. 9 Breech end power supply (a) Capacitors, (b) Inductor, (c) Ignitron, (d) Diode-triggered crowbar

The puff-switch details are shown in Figs. 10 and 11. The switch consisted of a pair of brass electrodes which passed through the gun body, 12 mm either side of the rails. The potential difference between these electrodes was that of the capacitor bank and the average potential was initially that of the gun rails. The principle of operation is that conducting matter, passing outwards through the puff-holes, causes an arc breakdown between the electrodes and the rails. The polycarbonate sleeves with 12 mm diameter holes opposite the puff-holes were intended to help confine the arc to the volume near the puff-holes. The electrodes were hollow and holes were drilled in their sides to allow high pressure gas from the arcs to escape. The O-ring seals were used to prevent venting downwards

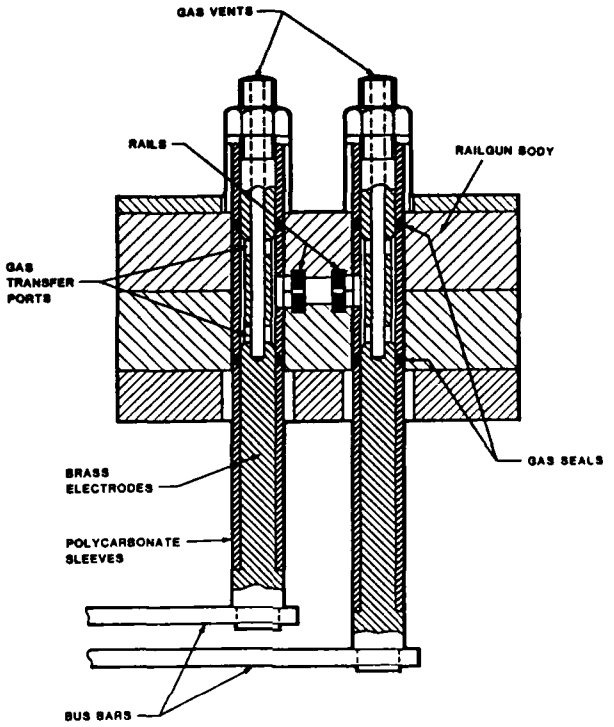

FIG. 10 Puff-switch details

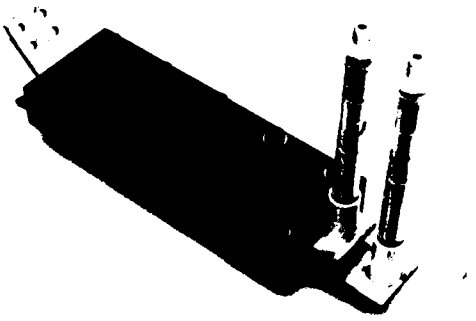

FIG. 11 Completed puff-switch

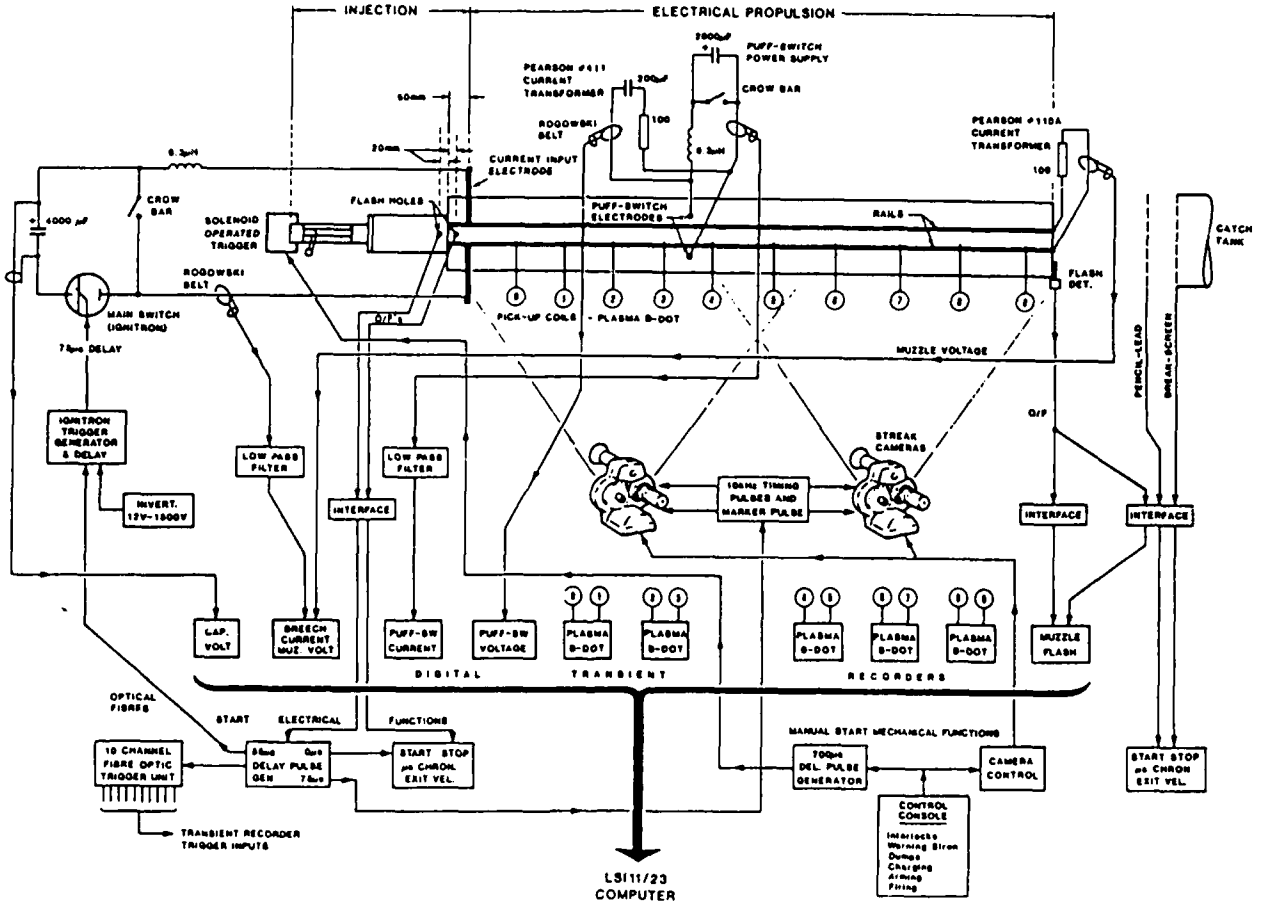

FIG. 12 Instrumentation of railgun

as this would cause "shorting" across the bus bars connecting the power source to the puff-switch.

The instrumentation used with the gun is shown in Fig. 12. Measurements were made of voltages and currents associated with the breech and puff-switched supplies, velocity of injection and of muzzle velocity. Ten magnetic pick-up ($\dot{B}$) coils were used. Two streak cameras were used to view the railgun via overhead mirrors. The two cameras had an overlapping field of view near the centre of the gun. Calibration of the streak records in terms of distance from the breech, was provided by the marker bars (Fig. 7) spaced every 100 mm. Time calibration was achieved by means of a 10 kHz timing light along the edge of the film. Seventeen digital transient-recording channels were used to record the data during the experiments. The data from the digital recorders was then transferred to a data storage and processing system based upon on LSI 11/23 computer.

The projectiles (Fig. 13) used in the experiments were made by nesting together pyramid-shaped mouldings of polycarbonate + polyethylene [9]. A piece of copper clad polyester film was inserted between the second and third pyramids from the rear in order to initiate the plasma arc. The mass of the accelerated portion, i.e. the first 7 pyramids, was 1.2 g. In the powder-only shot, magnetic strips were inserted either side of the projectile to provide magnetic pick-up coil data.

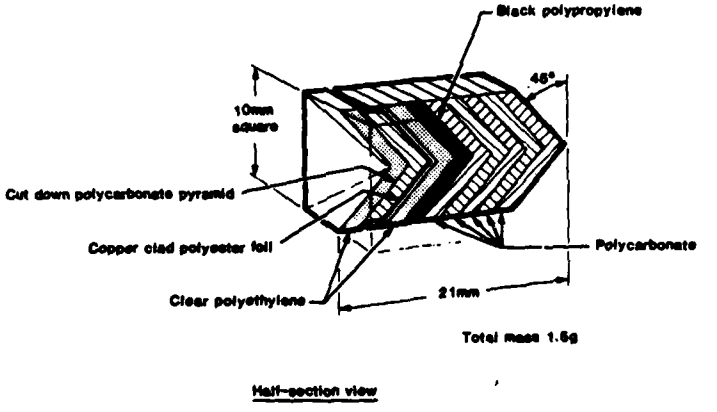

FIG. 13 Projectile construction - nested pyramids

2.3 Input Parameters of Experiments

The first puff-switch experiment was conducted with the breech capacitor bank charged to 6 kV, corresponding to 72 kJ stored energy. The puff-switched bank was charged to 4.5 kV, corresponding to 20 kJ stored energy. The puff-holes for this shot were 2 mm diameter.

In the second puff-switch experiment the breech supply was again 6 kV but the puff-switched supply was charged to 8 kV, corresponding to 64 kJ stored energy. The puff-holes for this shot were 0.38 mm diameter.

The reference shot, with the breech supply only, was conducted at 6 kV. The puff-hole diameters were 2 mm for this shot.

New sets of rails were used for each shot and new electrodes were used for each of the puff-switched shots.

The injector was loaded with a 7.62 mm cartridge filled with 1 g of T powder. It injected the projectile into the railgun at velocities in the range 1000 m/s to 1200 m/s.

All shots were conducted at atmospheric pressure.

3. RESULTS, ANALYSIS AND INTERPRETATION

3.1 Puff-Switch Operation

A rather low energy, 20 kJ, was used in the first puff-switch shot to minimize damage should the energy have discharged improperly. The switch in fact appeared to work quite well except that it commenced conduction early, apparently when the plasma leading edge was still about 130 mm from the puff-holes. A surprisingly large volume of luminous gas erupted from the puff-switch and afterwards its inner and outer surfaces were found to be coated with fine black powder. There was considerable erosion of the brass electrodes of the switch, in the region from where the arc to the rails had emanated (Fig. 14). The electrodes were slightly bent during the firing. On the bore sides of the rails (Fig. 15) the arc damage changed from fine streaks to a sandblasted appearance for about 70 mm on the breech side of the puff-holes, confirming that the second stage had commenced to conduct prematurely. Close to the puff-holes, and for a few centimetres on the muzzle side, there was almost no damage. Thereafter, the damage developed into a pattern of broad streaks with diverging feathery edges. These arc damage patterns are discussed further in Section 3.2.6. On the outer sides of the rails there was a considerable deposit of brass around the puff-holes.

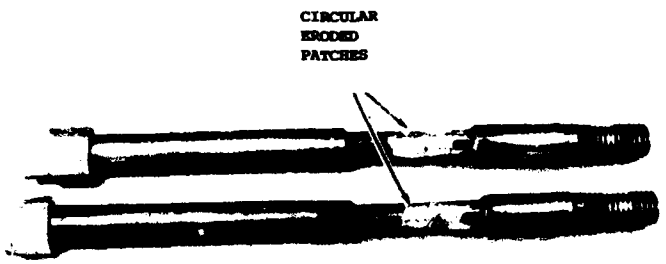

FIG. 14 Puff-switch electrodes after first puff-shot

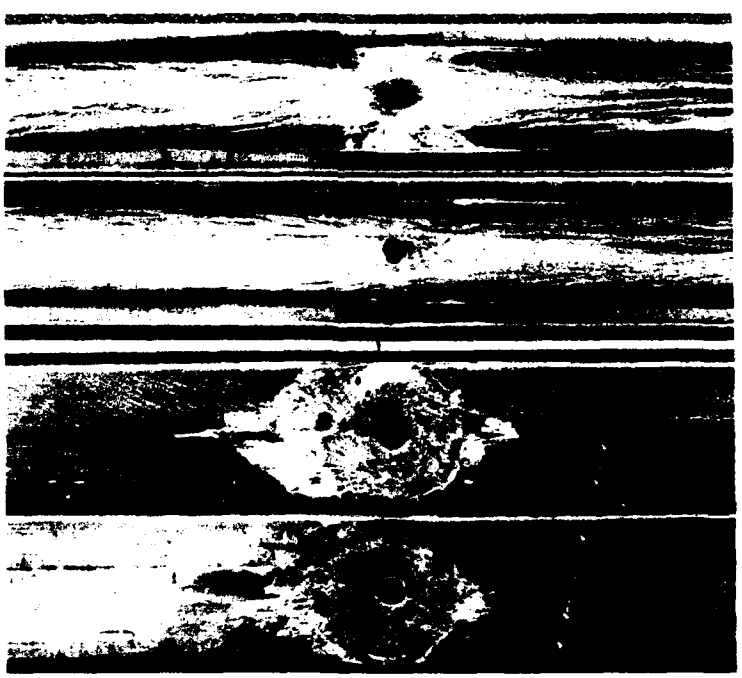

FIG. 15 Puff-hole region of rails after first puff-switched shot
Top: bore sides. Bottom: outer(puff-electrode) sides.
Left hand end is breech end

The projectile in this shot was injected at a velocity of about 1155 m/s and, if the projectile had the same velocity as the plasma leading edge as recorded on the streak photograph, it attained a peak velocity of about 2248 m/s. In the reference shot a peak velocity of about 2058 m/s was reached. These figures indicate that the 1.2 g projectile obtained about 1741 J from the 72 kJ stored by the breech power supply and about 491 J from the 20 kJ stored by the puff-switched supply. About 2.4% of the power source energy became projectile energy in each case. As will be shown later, much of the projectile energy was probably obtained from the explosive formation of the plasma rather than directly from the electrodynamic force. The velocity of the projectile at exit in the puff-shot was about 2100 m/s and in the reference shot it was about 1740 m/s.

The most likely reason for the early triggering of the puff-switch was thought to be that some conducting matter had by-passed the projectile. It was concluded that smaller puff-holes would greatly reduce the likelihood of the entry of such material. The large amount of gas from the electrodes and the violence of the arc also suggested that the holes were too large. For these reasons the second puff-switched shot was carried out with the puff-holes reduced to the diameter of the smallest practicable drill, viz. 0.38 mm. Sealing around the rails (using Silastic), from the breech to the puff-hole region, was also carried out to prevent leakage through gaps that might be created around the rails by the tendency of the high pressure plasma to push the halves of the body apart. New electrodes were installed in the puff-switch and the puff-switched capacitor bank was charged to 8 kV, corresponding to 64 kJ of energy. Based upon the performance of the first shot, it was anticipated that the projectile would emerge from the barrel at 3 km/s.

The result of the second puff-switch experiment was disappointing, although spectacular (Fig. 16). It made clear that the trial design of the puff-switch was unsuitable. The maximum velocity was about 2462 m/s, which again corresponds to 2.4% conversion of the energy of the puff-switched supply. Exit velocity was about 2315 m/s.

Despite the puff-holes having only 1/26 the area of those in the first experiment and the extra care taken in sealing around the rails, the switch triggered about 90 mm ahead of the plasma.

The operation of the puff-switch in this high energy second shot was also violent. A great quantity of luminous gas escaped from the electrodes and from between the halves of the body (Fig. 16). The polycarbonate sleeves and nuts and vent pipes were shattered and pieces were thrown up to 15 m from the gun. A piece of polycarbonate about 4 cm long spalled from the bore surface between the puff-holes. The halves of the body were forced apart in the puff-hole region and covered with soot and condensed copper from the rails (Fig. 17). Black soot completely covered the puff-switch surfaces. The puff-switch electrodes were badly bent (Fig. 18). Brass was deposited on the insides of the rails as well as on the outer sides (Fig. 19), and on their edges. The sealant on the rail edges was charred. Arc-damage marks between the busbars beneath the puff-switch suggested that arc pressure drove plasma downwards past the O-ring seals and "shorted" the busbars.

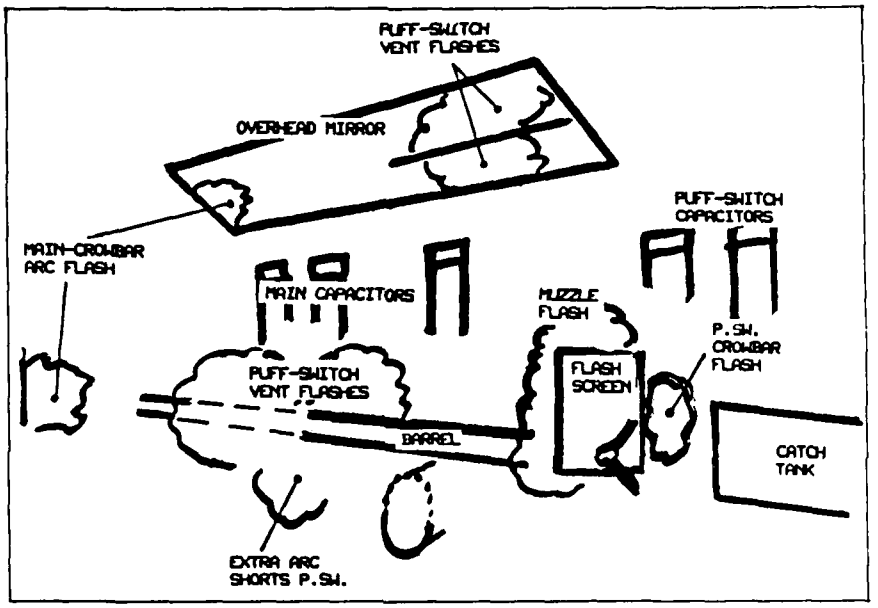

FIG. 16 Video frames from a recording of the second puff-switched firings. The first four consecutive frames are shown on the following pages.

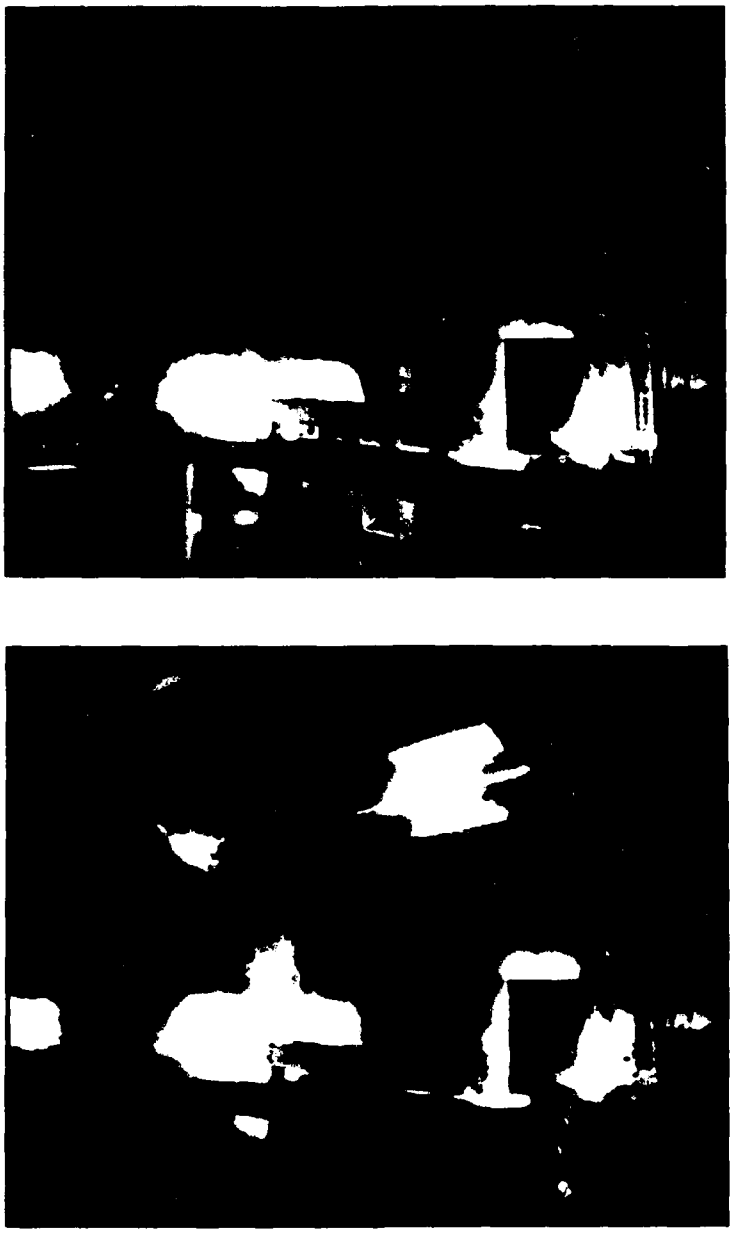

FIG. 16 (Cont.) Firing of the second puff-switched shot.
(First and second frames from the video tape.)

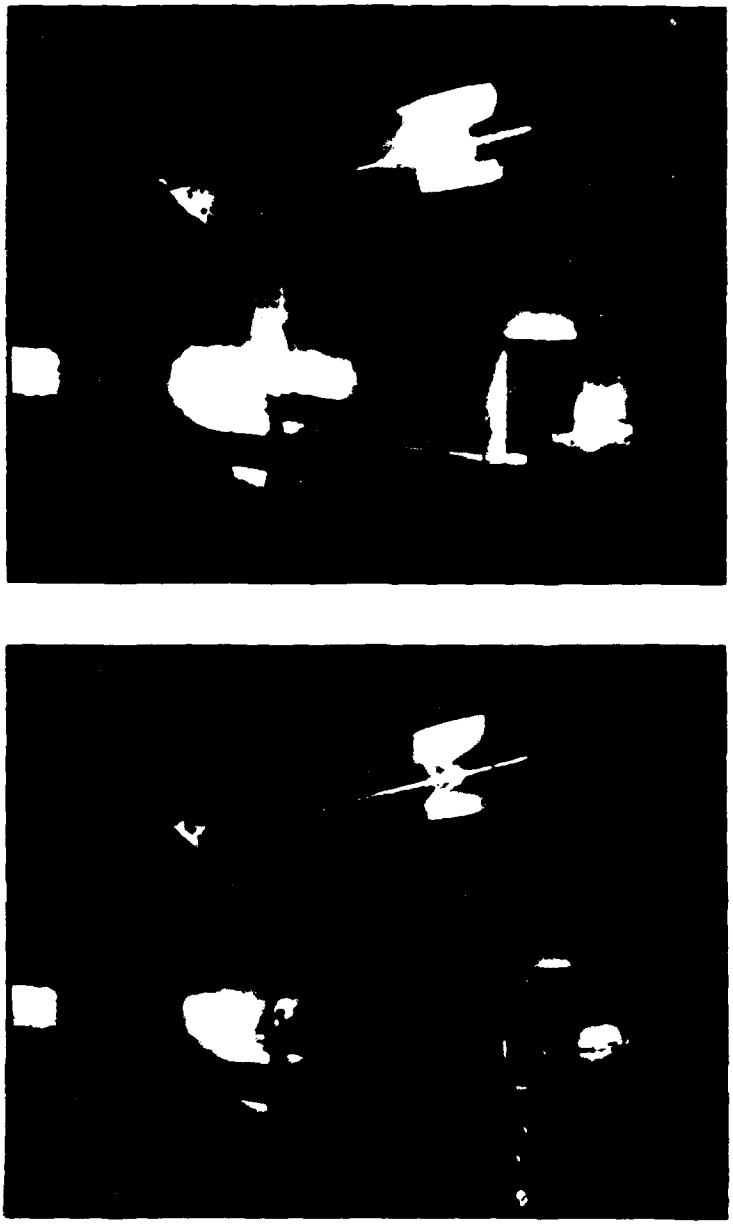

FIG. 16 (Cont) Firing of the second puff-switched shot.
(Third and fourth frames from the video tape.)

FIG. 16 (Cont) First two (of four) 16 gauge duralumin target plates at 25 mm spacing.
The fourth plate was not penetrated but was deeply indented.

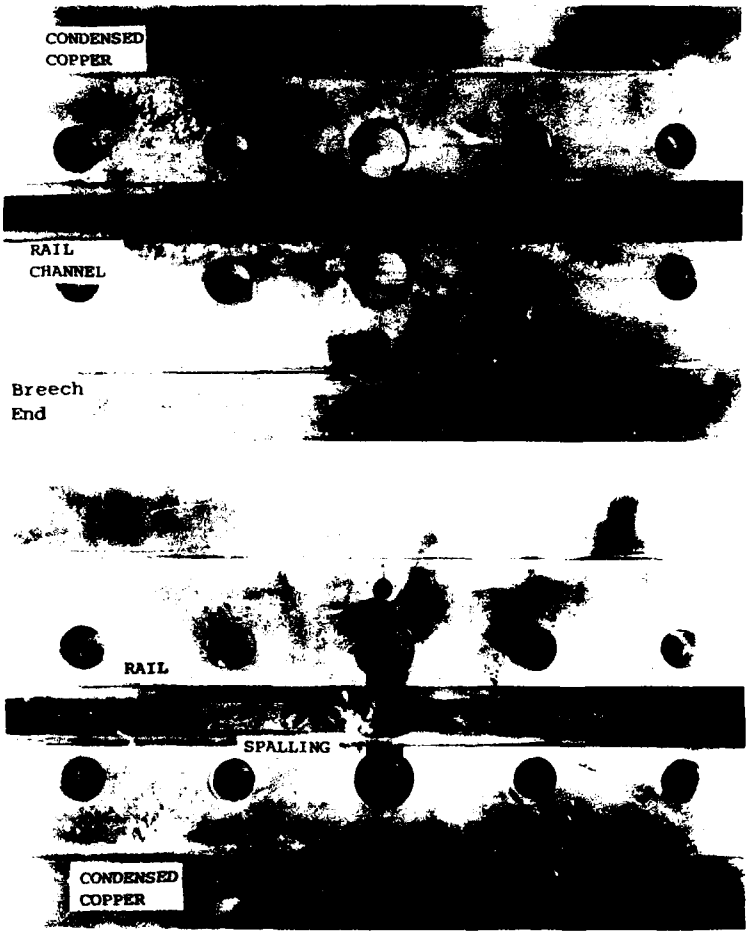

FIG. 17 Halves of gun body after second puff-switch shot - puff-switch region

FIG. 18

Puff-switch electrodes

after second shot

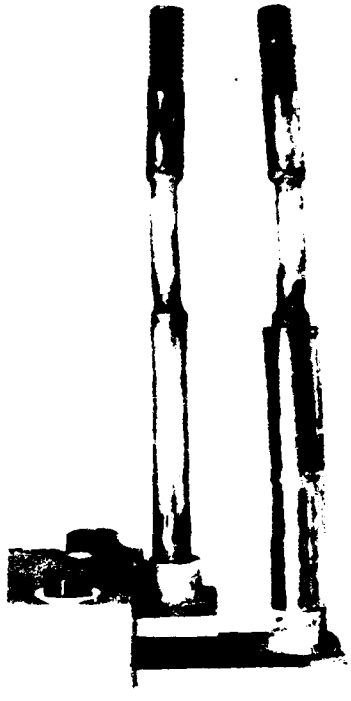

FIG. 19 Rails, second puff-switched shot
Top: bore sides. Bottom: outer sides

3.2 Presentation and Study of Data

The streak photographs and graphs and other information from the experiments are given below together with detailed analysis and interpretations.

3.2.1 Streak photographs

Streak photographs show the position of the plasma on the vertical axis (the short axis) and time on the horizontal axis. The streak records from the reference shot and the two puff-switched shots are given in Figs. 20-22.

The vertical calibration is given by the 100 mm spaced marker bars superimposed on the streak, and the horizontal calibration is given by the 100 μs interval between timing light pulses recorded on the edge of the film. On the other edge of the film is a timing light pulse which is precisely located with respect to the triggering of the ignitron used in the breech power supply. This enables the true zero time position on the streak to be found, i.e. the time at which electric current commenced to accelerate the projectile.

Velocity can be found by measuring horizontal distances between the 100 mm bar positions and using the time calibration factor, but as discussed in the next Section it is more accurate to obtain the velocity from the slope of the streak record.

Provided that the streak photograph is a record of only the hot, current conducting, portion of the plasma and not of lower temperature gases and glow from the body, the length of the moving plasma armature is given by the vertical distance through the streak. The selection of film type (Kodak Tri X) and of filters to control the exposure has been discussed previously [15]. The muzzle end streak of the reference shot (Fig. 20) shows the effect of overexposure. An ND 1.0 filter was used on the camera in this case instead of the usual ND 2.0 filter. Image analysis equipment with false colour presentation of light intensities was used to study the negatives and to supplement the prints obtained by normal methods. Image analysis (Fig. 23) supports the belief that the breech end streaks in the reference shot and the first puff-switch shot are reasonable records of the moving plasma armature. From these it appears that the armature length steadily increases from zero to 70 100 mm. The overexposed second half of the reference shot streak apparently shows much greater plasma length, but may also be indicative of lower temperature, low velocity portions of the plasma that are left behind the armature, and also of afterglow of the body.

In the puff-switch firings the horizontal streak below the main streak indicates that portion of the plasma remained as an arc between the puff-holes in the rails for about 100 μs and then extinguished as the current within it diminished.

Fig. 22 also shows that in the second puff-switched shot the plasma slowed as it approached the puff-hole region. Evidently some of the puff-switched current flowed towards the breech through the approaching main plasma, thereby causing a force in the reverse direction and slowing the

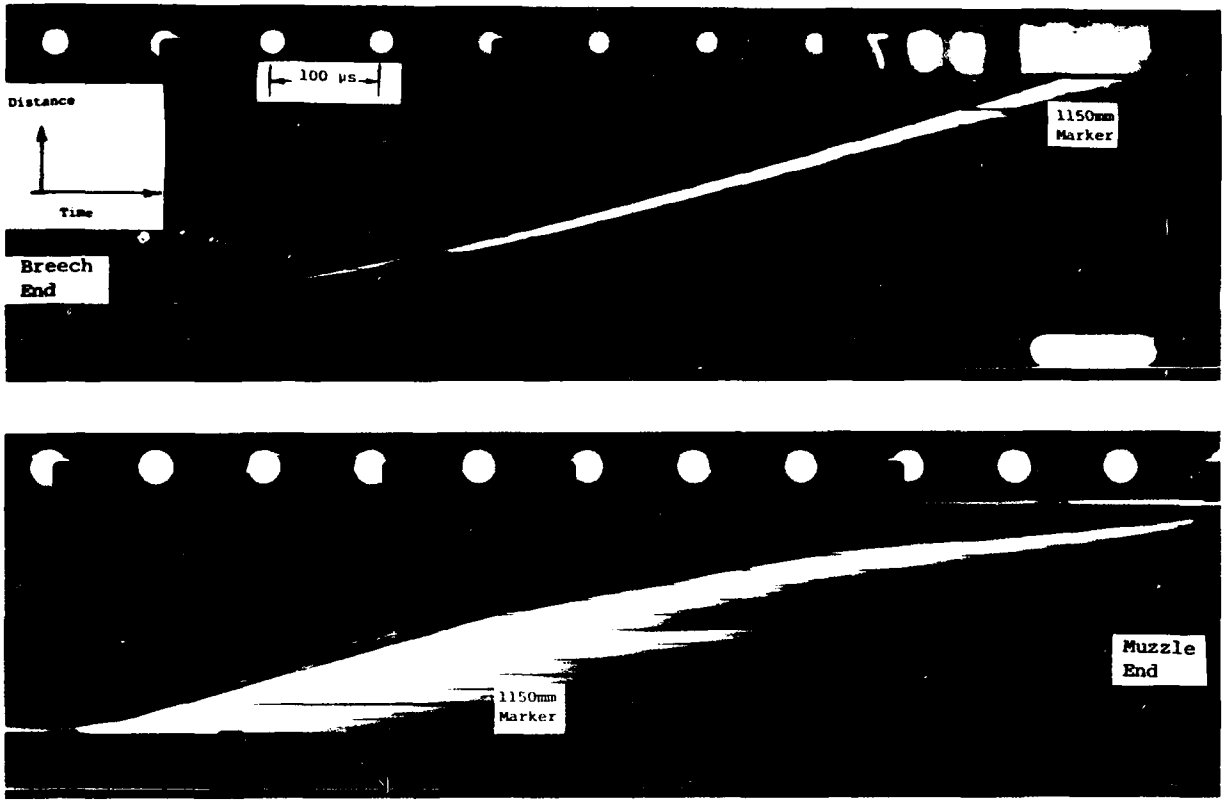

FIG. 20 Streak photographs - Reference shot Muzzle end streak over-exposed
On this and other records marker bar at 1150 mm is double width

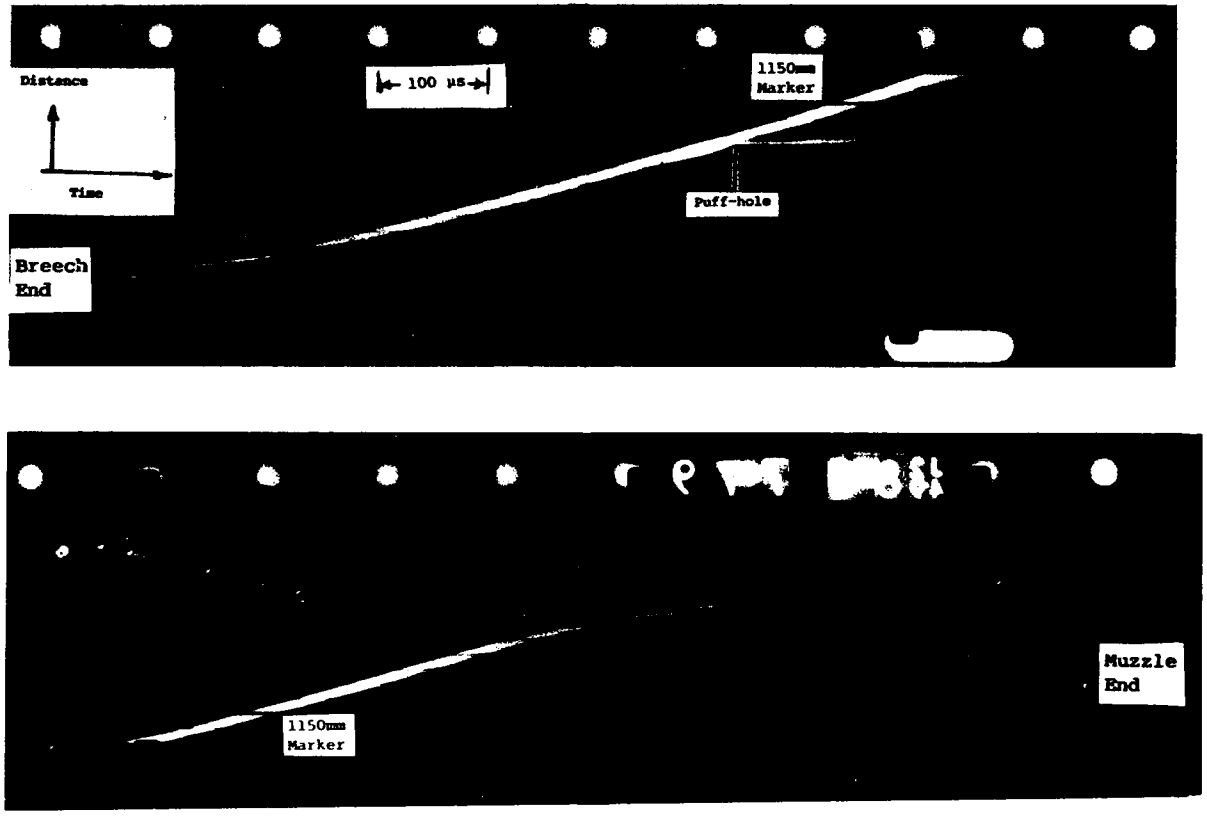

FIG. 21 Streak photographs - First puff-switched shot

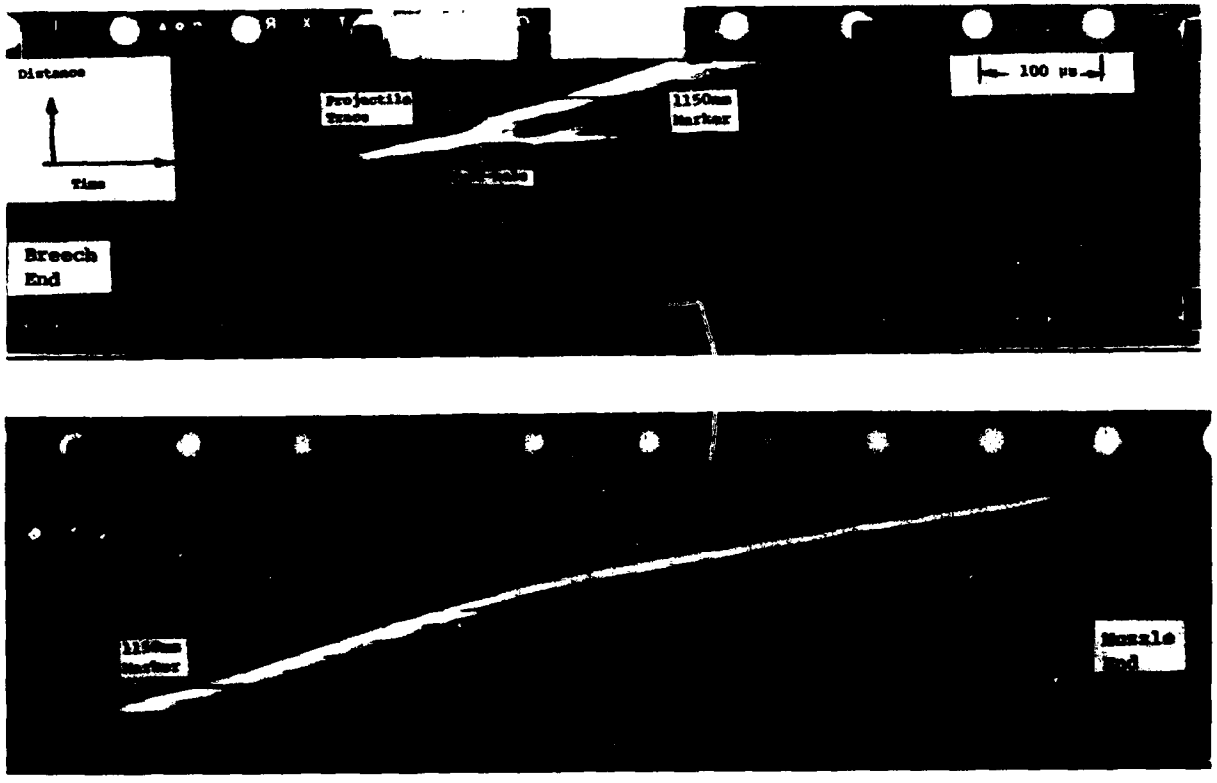

FIG. 22 Streak photographs - Second puff-switched shot Breech end streak was seriously underexposed.

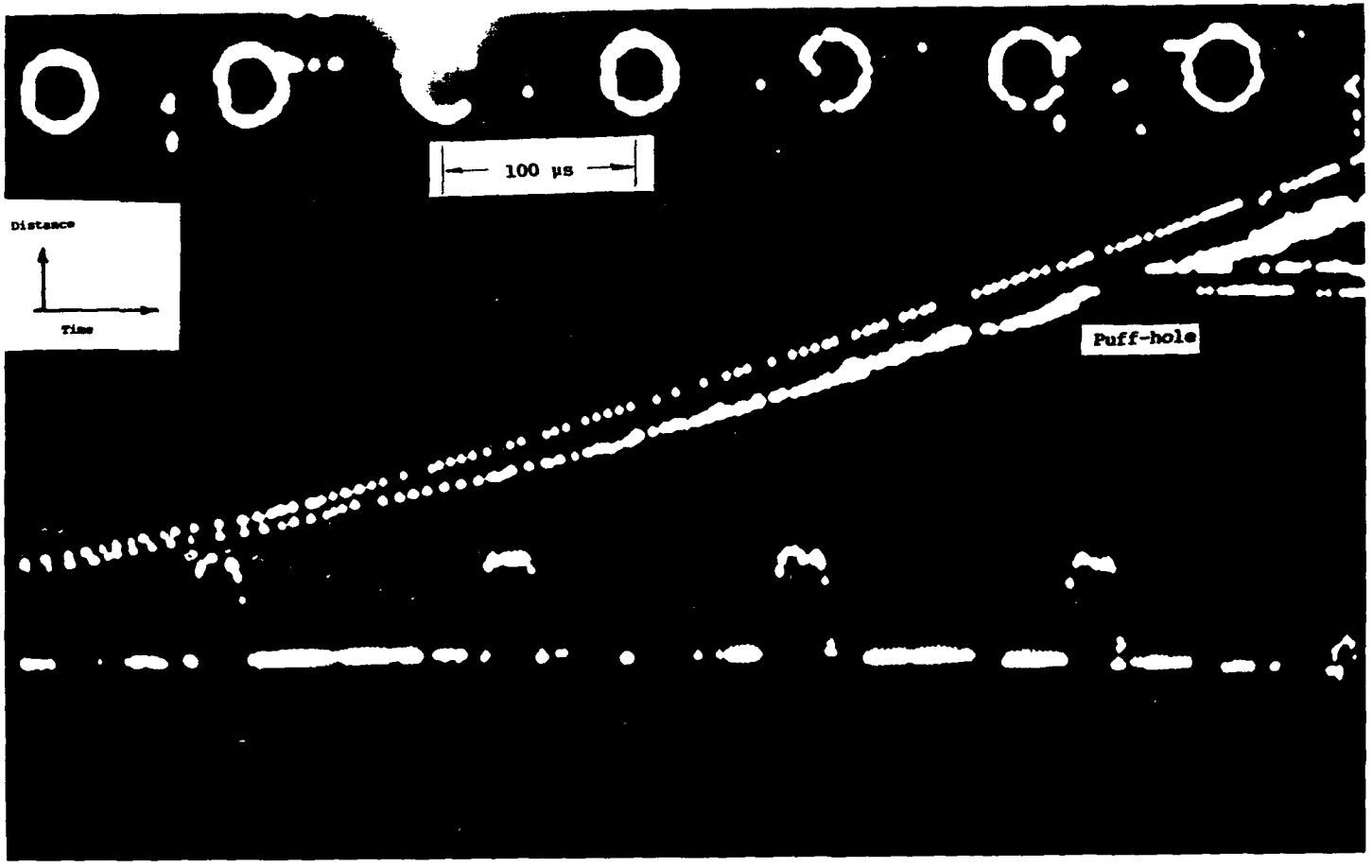

FIG. 23 *Image analyser presentation of breech end streak in first puff-switched shot*

plasma. A faint line can be seen continuing at constant velocity in the puff-switch region, indicating that the projectile, unlike the plasma, did not slow down. The steep discontinuity in the streak record shows that soon after the projectile had passed the puff-holes, the plasma accelerated to about 5200 m/s until it caught up with the projectile.

All the streaks show that the plasma slowed considerably and diminished in intensity towards the muzzle end. These effects may be due to increasing plasma mass and decreasing current. In the reference shot and the first puff-switched shot there is marked slow-down and plasma weakening when the current falls to about 40 kA. The deterioration of the plasma correlates with the falling back of current from the plasma leading edge and with the appearance of deep arc-pits on the rails (Sections 3.2.4 and 3.2.6).

Whilst the leading edge of the plasma is increasing in velocity it produces a distinct line on the streak photograph. This implies that the plasma is against the projectile and that the projectile velocity is that of the leading edge of the plasma. As soon as the leading edge velocity decreases the edge becomes less distinct, implying that the projectile has continued at the higher velocity and has separated from the plasma.

3.2.2 Velocities

Velocities obtained from the leading edges of the streak photographs of the reference and puff-switched experiments are given in Figs. 24 and 25.

The velocity of the projectile in the powder-only shot, as determined by pick-up coils, is also plotted in Fig. 25.

The method used to determine the leading edge velocity was to measure the slope of the leading edge and to use the relationship:

$$v = \frac{A}{B} \tan \alpha ,$$

where v is the velocity, A and B are the distance and time calibration factors and α is the slope angle. Enlarged prints, about 1 m long, enabled the slopes to be measured to within about 1/3 of a degree, corresponding to about $\pm$ 2% uncertainty in velocity. The slope method is more accurate than measuring the horizontal and vertical distances because the low slope angles ($10-17^{\circ}$) make it difficult to determine the horizontal lengths to within 5 to 10%.

The velocity graphs show that the plasma suddenly failed as a propulsion means after about 1 ms and that the gun was too long for the energy supplied. Figure 25 shows that a length of about 1500 mm would have been a better match. The sudden failure of the plasma suggests that there is a critical parameter, or group of parameters, which controls switching from one plasma state to another.

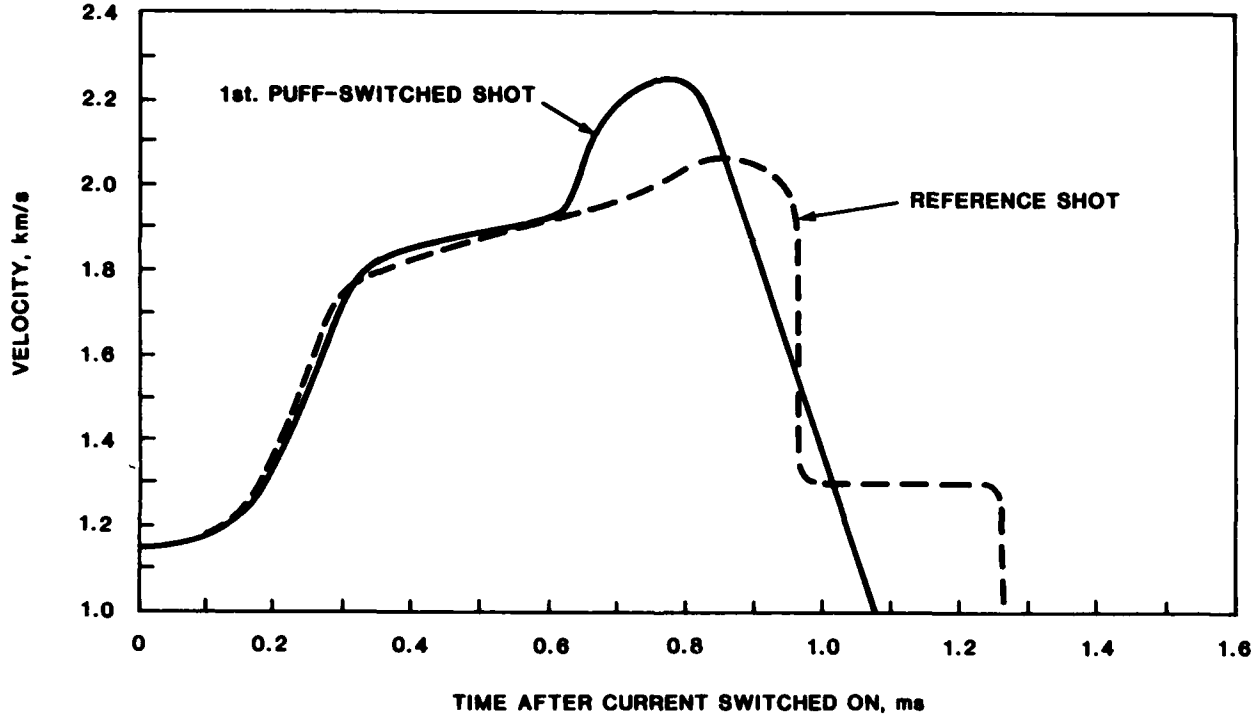

FIG. 24 Velocity of plasma leading edge versus time

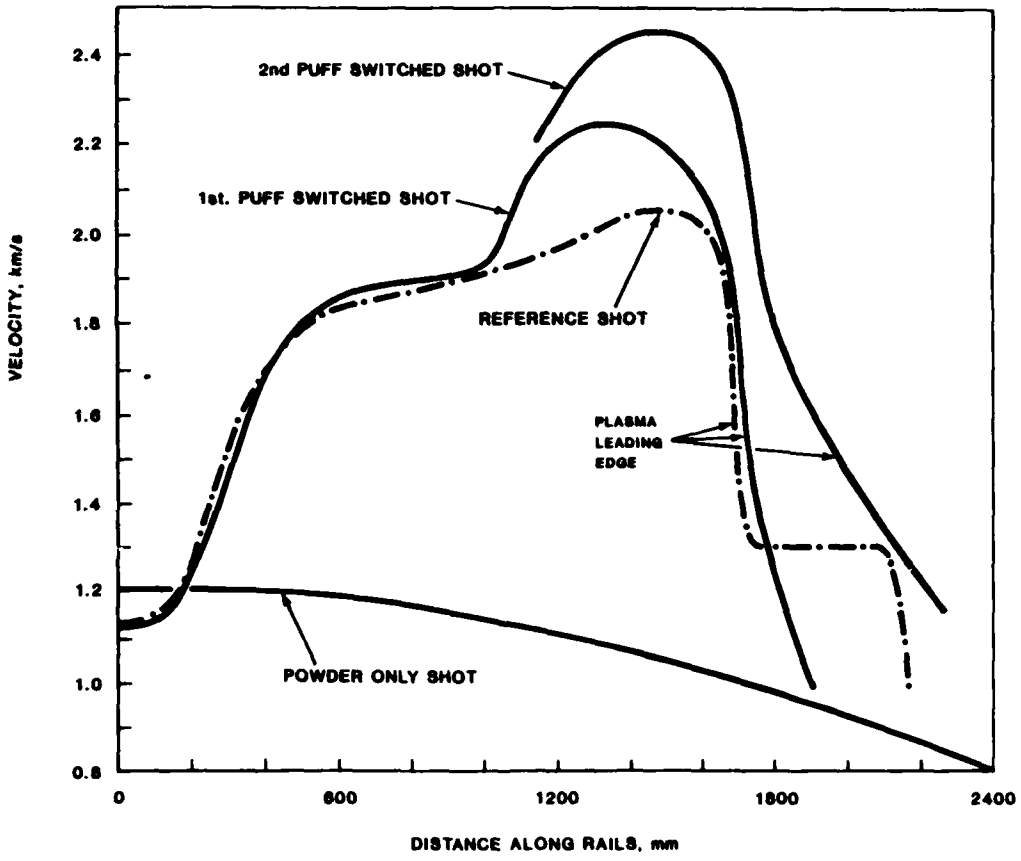

FIG. 25 Velocities of plasma leading edge in puff-switched shots and of projectile in powder-only shot

The injection, maximum and exit velocities of the projectile in the four shots were:

Velocities (m/s)

Shot	Injection	Maximum	Exit
Powder-only	1212	-	794
Reference	1155	2058	1923
1st Puff-Switched	1155	2248	2100
2nd Puff-Switched	1000	2462	2315

The exit velocities were measured over a 500 mm flight path in air between the muzzle and a catch tank.

The velocity plot of the powder-only shot (Fig. 25) shows that the powder gun gases did not continue to accelerate the projectile after it entered the railgun. It also shows that friction and air load caused the projectile velocity to decrease continuously from 1212 m/s to 794 m/s from about 600 mm to the end of the gun. The loss of velocity is greater than that of the other three shots. In the reference shot the velocity loss from the maximum of 2058 m/s at 1500 mm was 135 m/s compared with a velocity loss of 250 m/s over the same distance in the powder-only shot. In the puff-switched shots the velocity losses were 148 and 147 m/s. The fact that the decreases were smaller in all electrical shots implies that the plasma was exerting pressure upon the projectile until the projectile left the barrel, even when the light emitting region of the plasma was well behind the projectile.

3.2.3 Currents and Voltages

The measured breech supply (Main Supply) currents and puff-switched currents for the three electrical shots are shown in Figs. 26-30. The sums of the breech supply and puff-switched currents are also plotted in Figs. 28 and 30. The breech supply and puff-switch voltages are given in Figs. 31-35 and the muzzle voltage record for the reference shot is given in Fig. 36. Muzzle voltage records were not obtained in the puff-switched shots due to failure of the recorders to trigger.

Time on these records is measured from the pre-triggered start of the transient recorders and zero time is about 143 μs prior to switch-on of the breech current.

From the current records it can be seen that, for the puff-switched shots, the breech current rose to a peak value of about 114 kA in the expected sinusoidal fashion in about 250 μs. The peak current corresponds to about 41 kJ stored by the inductor, compared to lossless values of 150 kA and 72 kJ. About 30 kJ was thus consumed in plasma initiation, the ignitron and circuit resistances.

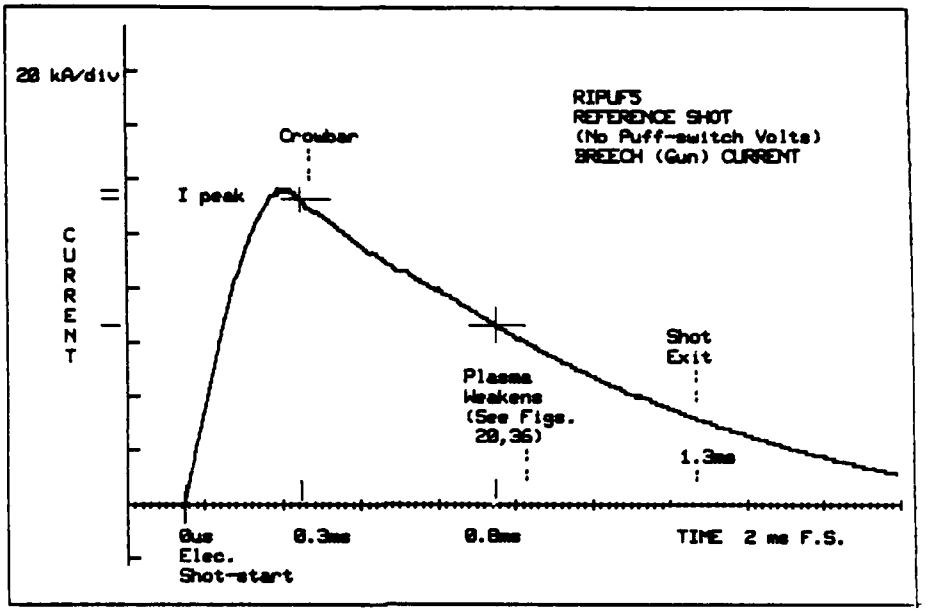

FIG. 26 Breech supplied current, reference shot

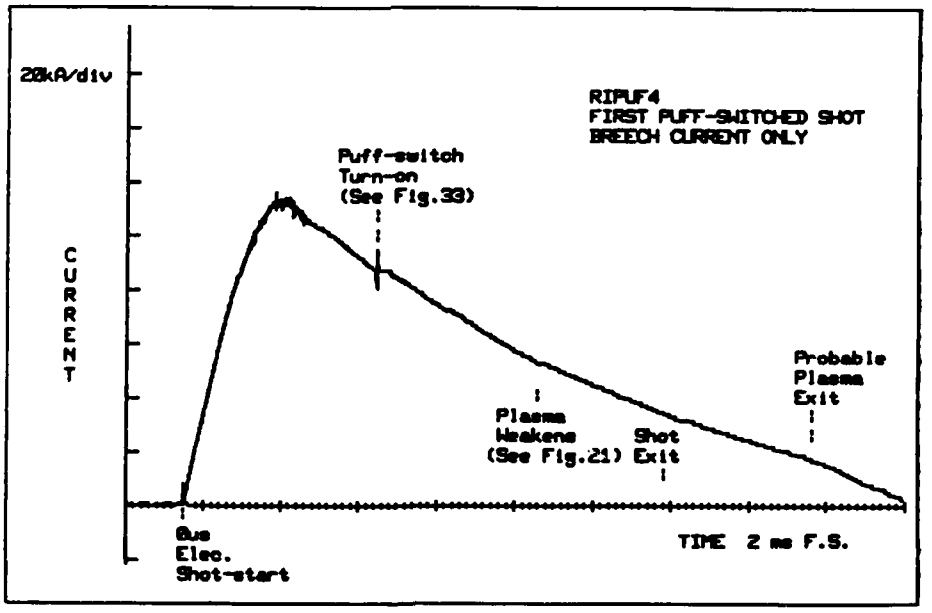

FIG. 27 Breech supplied current, first puff-switched shot

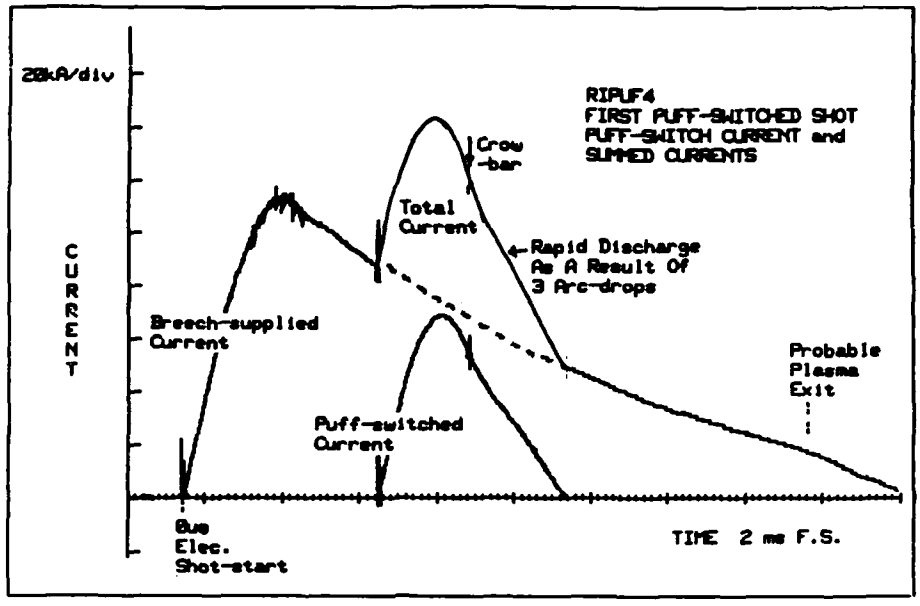

FIG. 28 Puff-switched current and sum of breech and puff-switched currents - first puff-switched shot

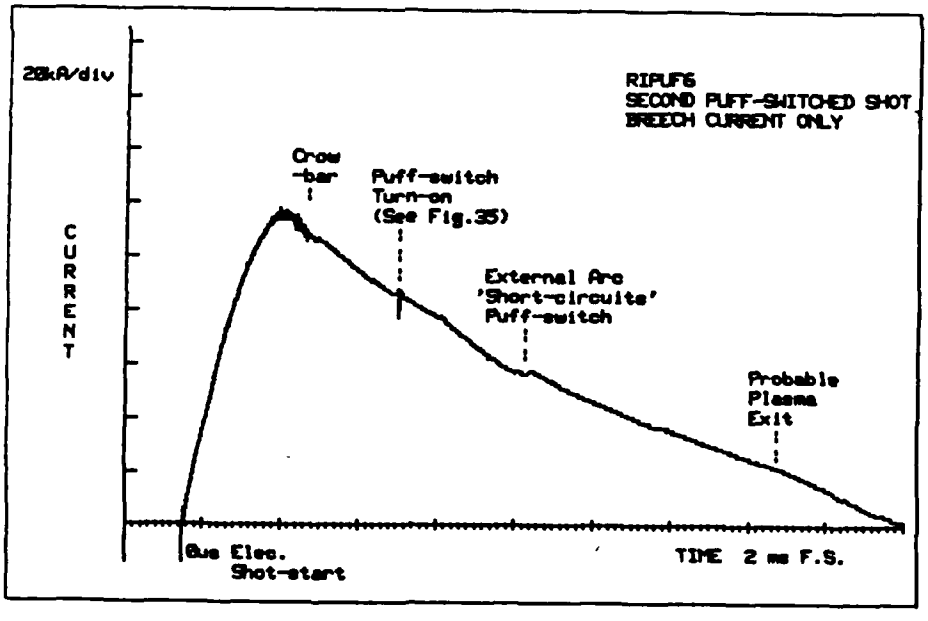

FIG. 29 Breech supplied current - second puff-switched shot

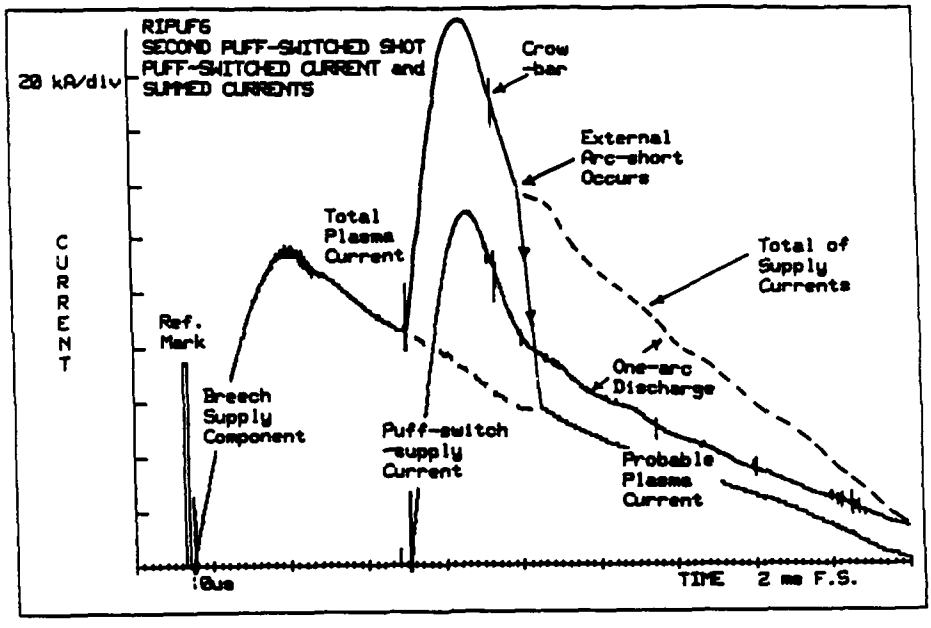

FIG. 30 Puff-switched current and sum of breech and puff-switched currents - second puff-switched shot

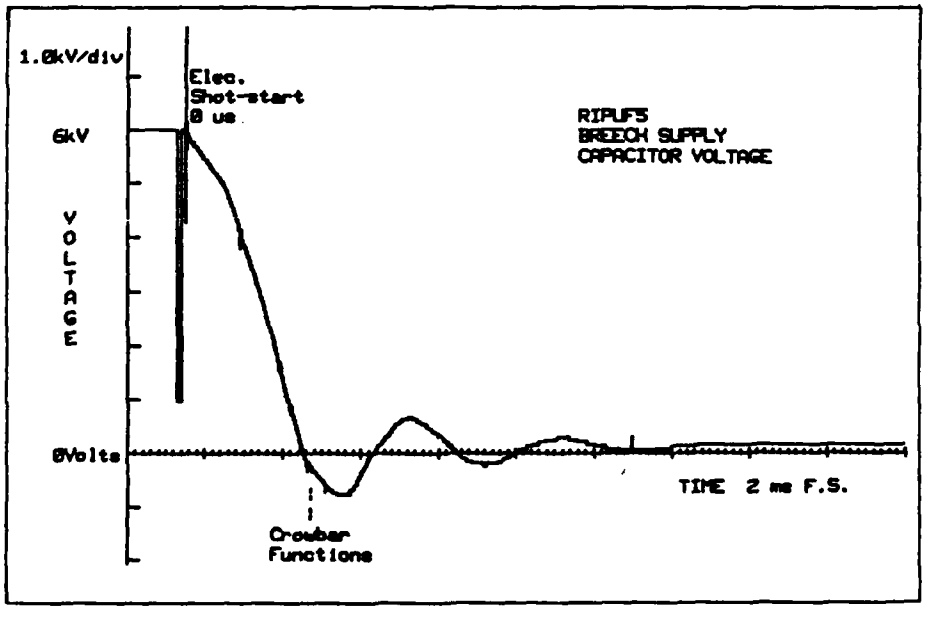

FIG. 31 Breech capacitor bank voltage - reference shot

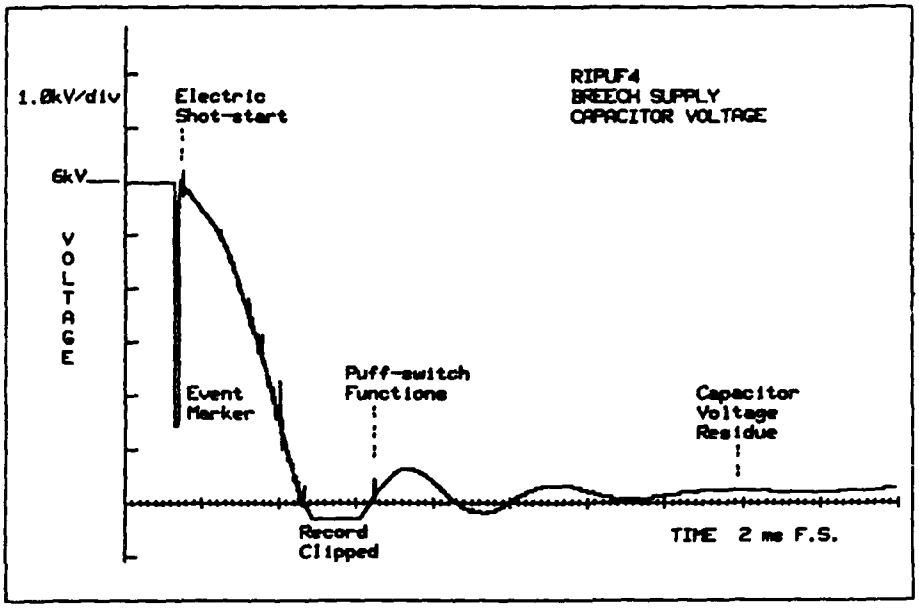

FIG. 32 Breech capacitor bank voltage - first puff-switched shot

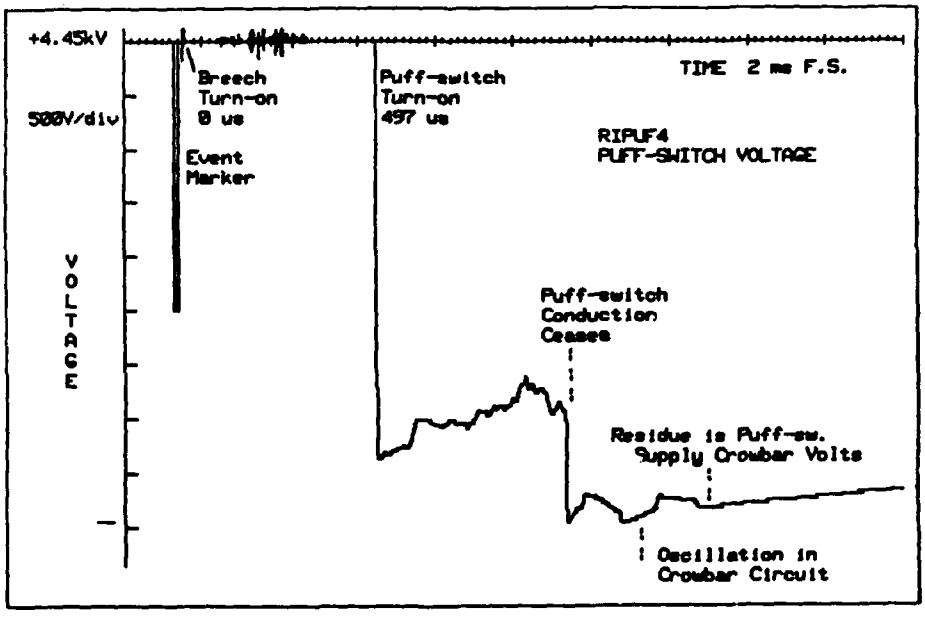

FIG. 33 Puff-switch inter-electrode voltage - first puff-switched shot

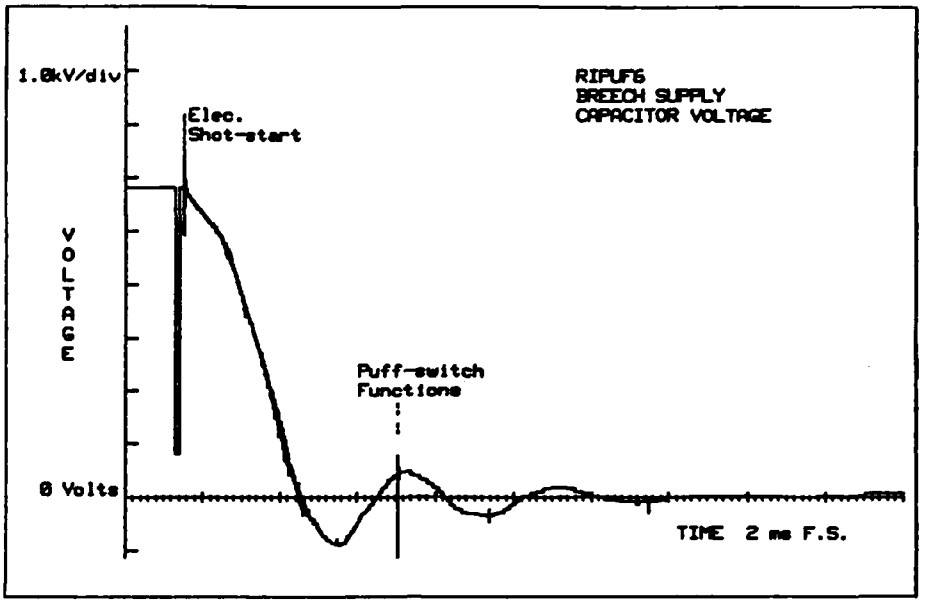

FIG. 34 Breech capacitor bank voltage - second puff-switched shot

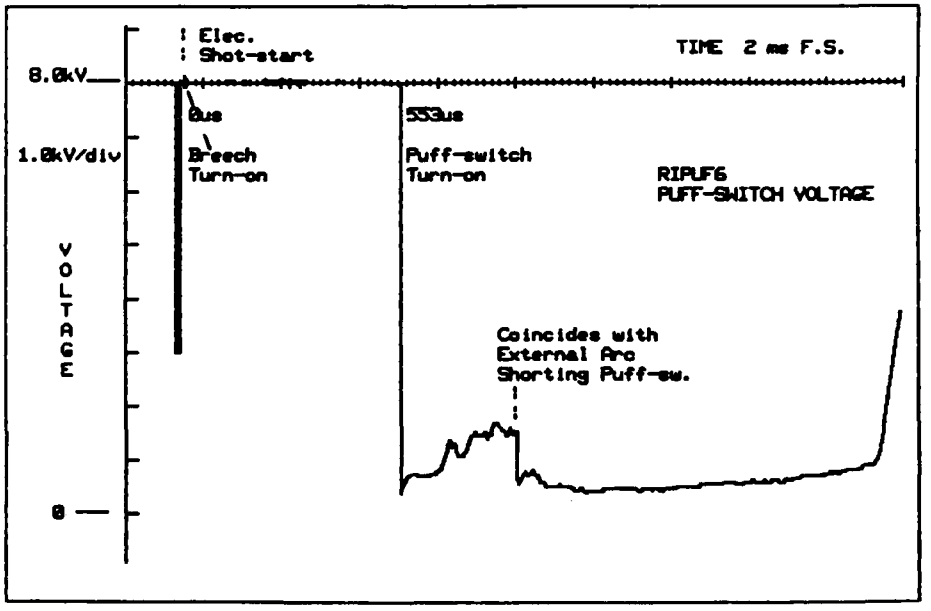

FIG. 35 Puff-switch inter-electrode voltage - second puff-switched shot

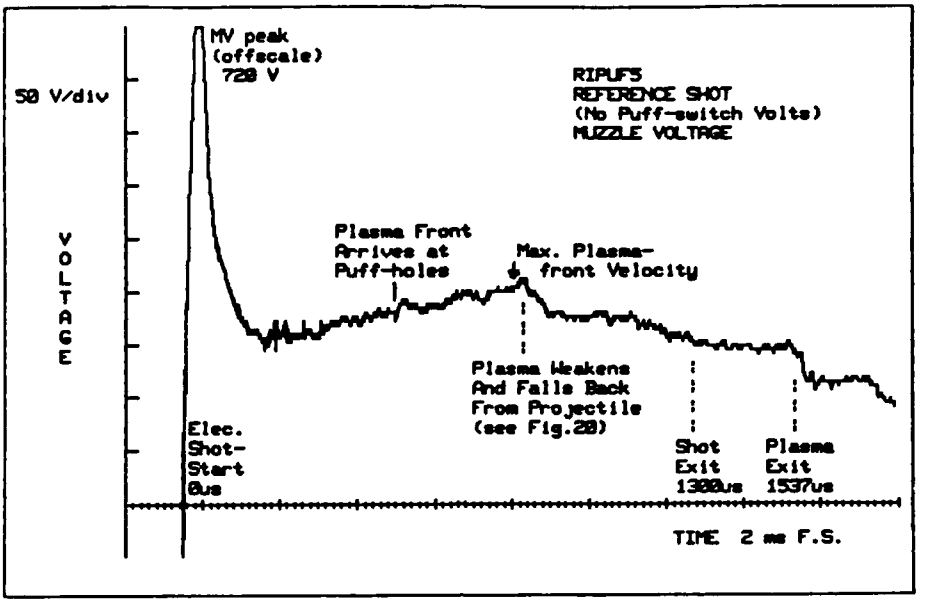

FIG. 36 Muzzle voltage - reference shot

The fall of voltage at the puff-switchs enables the exact times of puff-switch triggering to be determined as 497 μs and 553 μs after the turn-on of the breech supplies. By plotting these times on enlarged calibrated streak records it was found that in the first puff-switch experiment the puff-switch triggered when the leading edge of the plasma was still 130 mm from the puff-holes and that in the second puff-switch experiment triggering occurred when the leading edge was still 90 mm from the puff-holes.

The puff-switched currents decline from their peaks much more rapidly than do the breech-supplied currents. The rapid decline is probably due to the rail-to-electrode arc drops in the puff-switch and indicates that this simple scheme would be inefficient even if it worked well in other respects. In the second puff-switch shot the puff-switched current-time curve suddenly assumes a gradient similar to that of the breech supply. At the same time the puff-switched voltage rapidly falls. An explanation for this behaviour is that at this time an arc struck between the bus bars beneath the puff-switch and thus partly short circuited the rail-to-electrode arcs.

A muzzle voltage record was obtained for only the reference shot (Fig. 36). It clearly shows the foil explosion and the point at which the plasma fails as a propulsion means. The usual rise in voltage when the plasma leaves the muzzle does not occur in Fig. 36, because by this time practically all the energy had been dissipated.

3.2.4 Magnetic Pick Up Coils

Magnetic pick-up coils (also called $\dot{B}$ coils or position coils) give information about plasma length and the location and distribution of current in the plasma. The pick-up coils (Fig. 8) comprised ten turns on a 5 mm diameter former and were inserted into the polycarbonate body midway between the rails. The centre of the turns was about 7.5 mm beneath the bottom of the bore and the turns were oriented to link the plasma flux and but not the rail flux, ie. the coil axis was parallel to the barrel axis. Coil locations were 200, 400, 600, 800, 1000, 1250, 1500, 1750, 2000 and 2250 mm measured from the centre of the current input electrodes at the breech.

Sample pick-up coil traces are given in Figs. 37-43. Figure 37 shows the seven waveforms obtained in the powder-only shot in which magnetic strips were inserted into the projectile. (These strips were cut from a calendar designed to adhere to a refrigerator.) Figures 38 and 39 show the ten waveforms obtained in the reference shot; Figures 40 and 41 show the eight waveforms obtained in the first puff-switched shot and Figures 42 and 43 show the eight waveforms obtained in the second puff-switched shot.

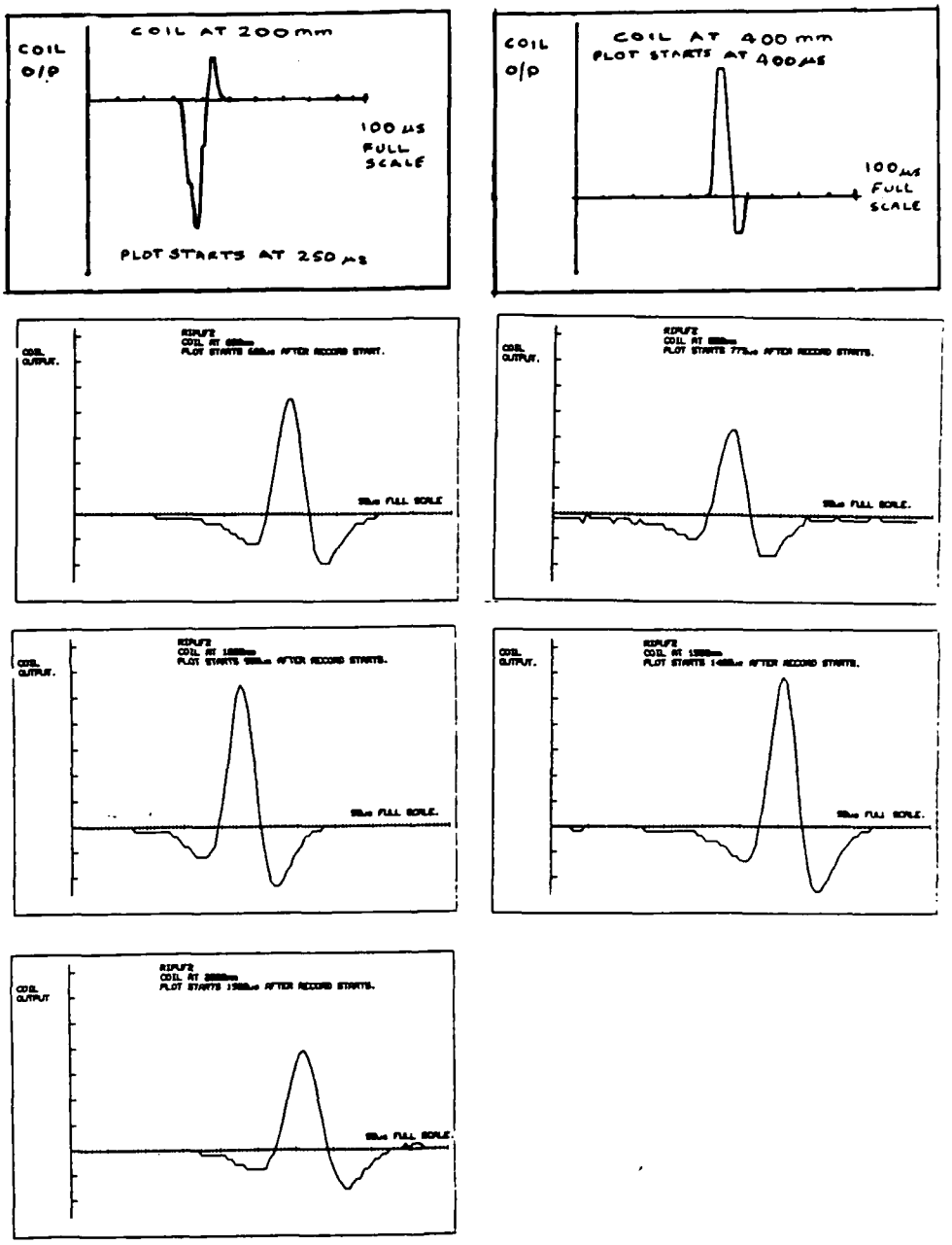

FIG. 37 Pick-up coil outputs, powder-only shot, using projectile with magnetic inserts

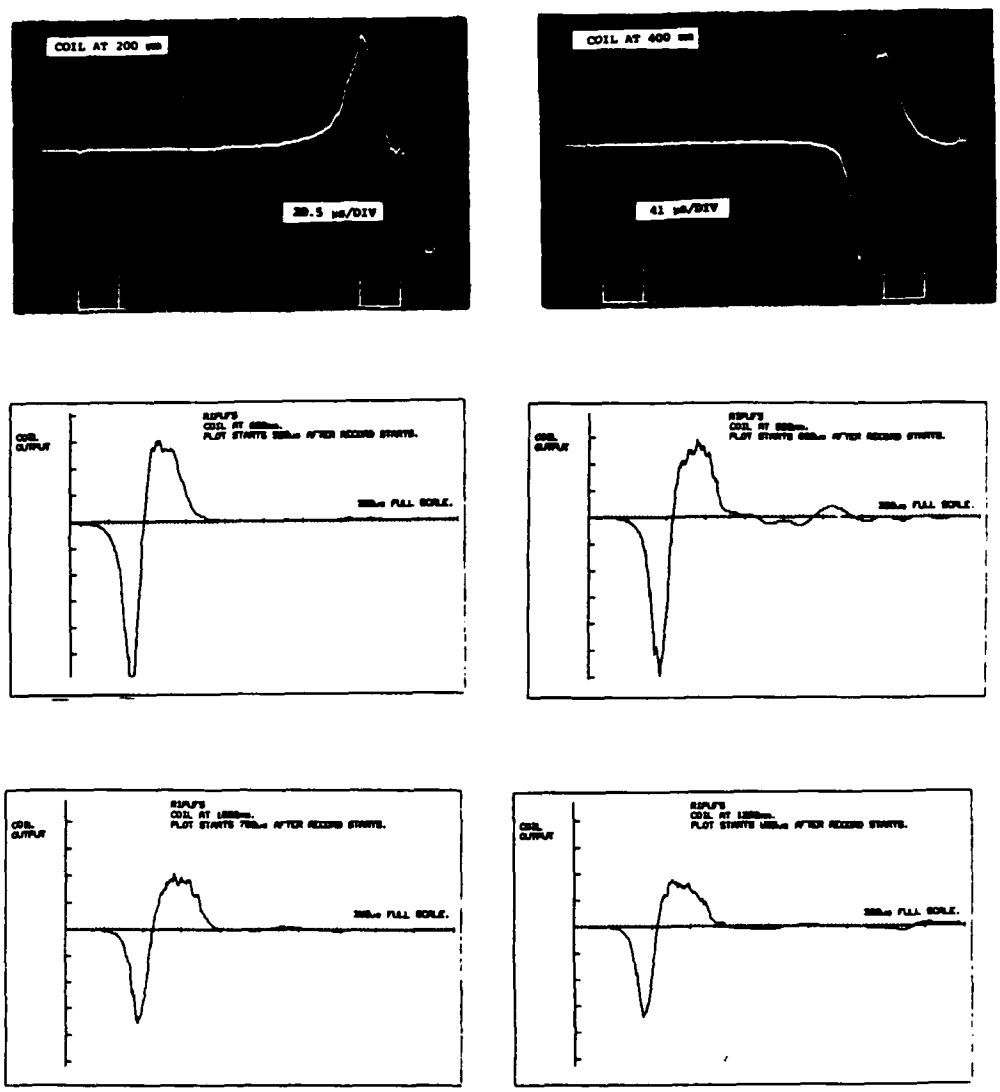

FIG. 38 Pick-up coil output - reference shot (Polarity of waveforms is arbitrary because of the difficulty of identifying starts and finishes of turns).

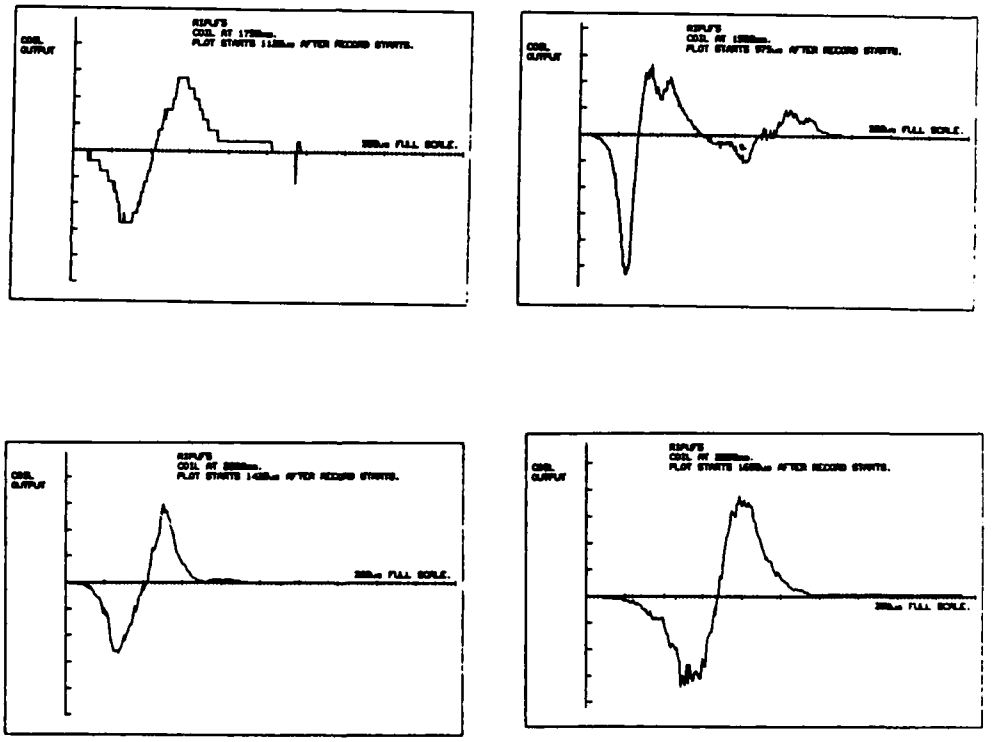

FIG. 39 Pick-up coil outputs - reference shot, continued

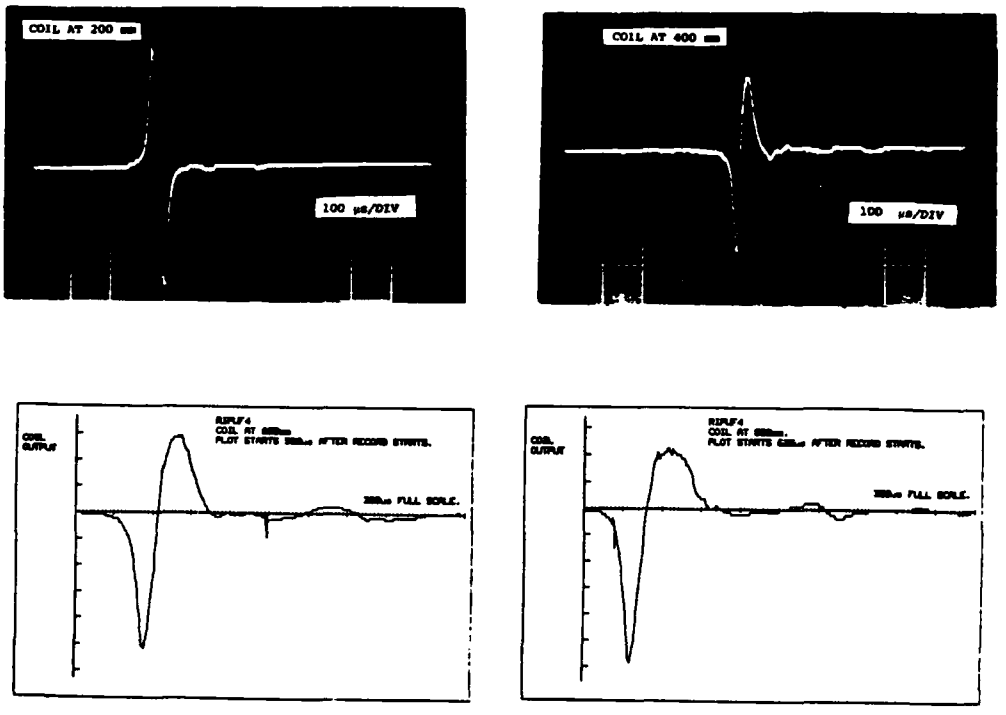

FIG. 40 Pick-up coil outputs - first puff-switched shot

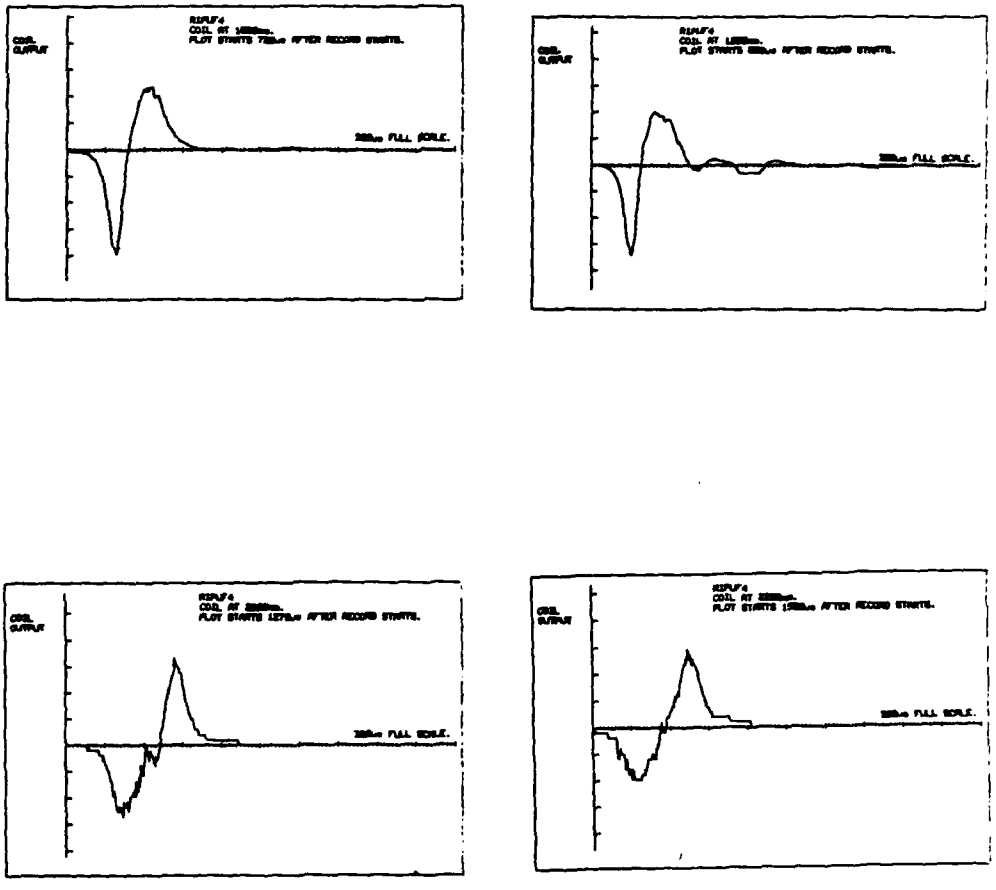

FIG. 41 Pick-up coil outputs - first puff-switched shot, continued

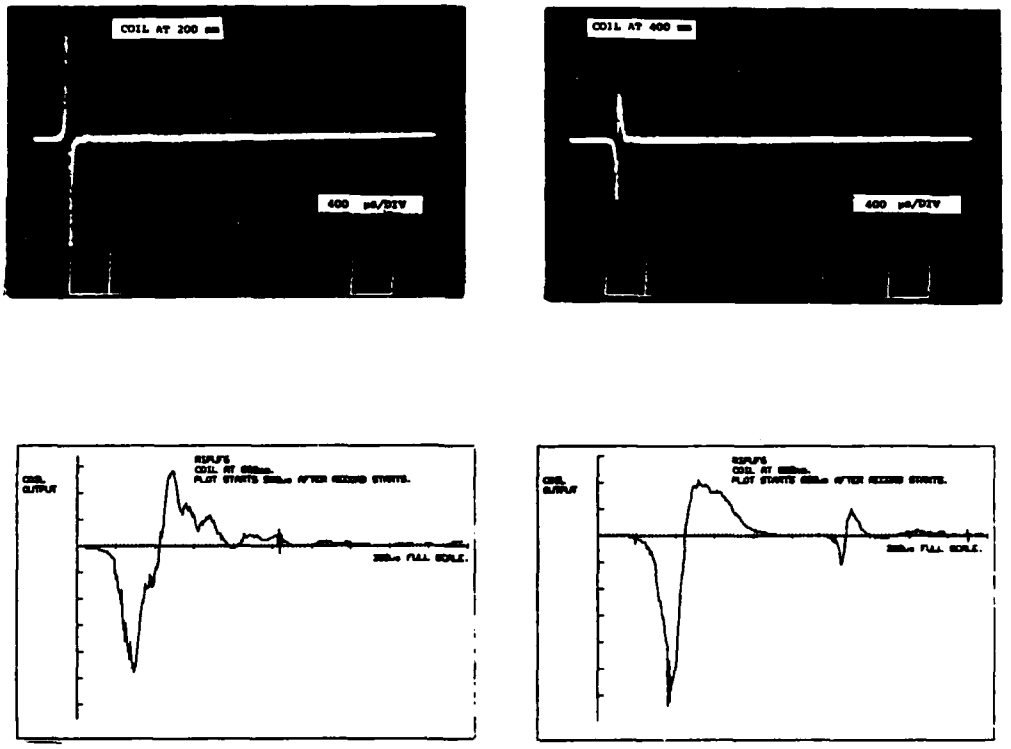

FIG. 42 Pick-up coil outputs - second puff-switched shot

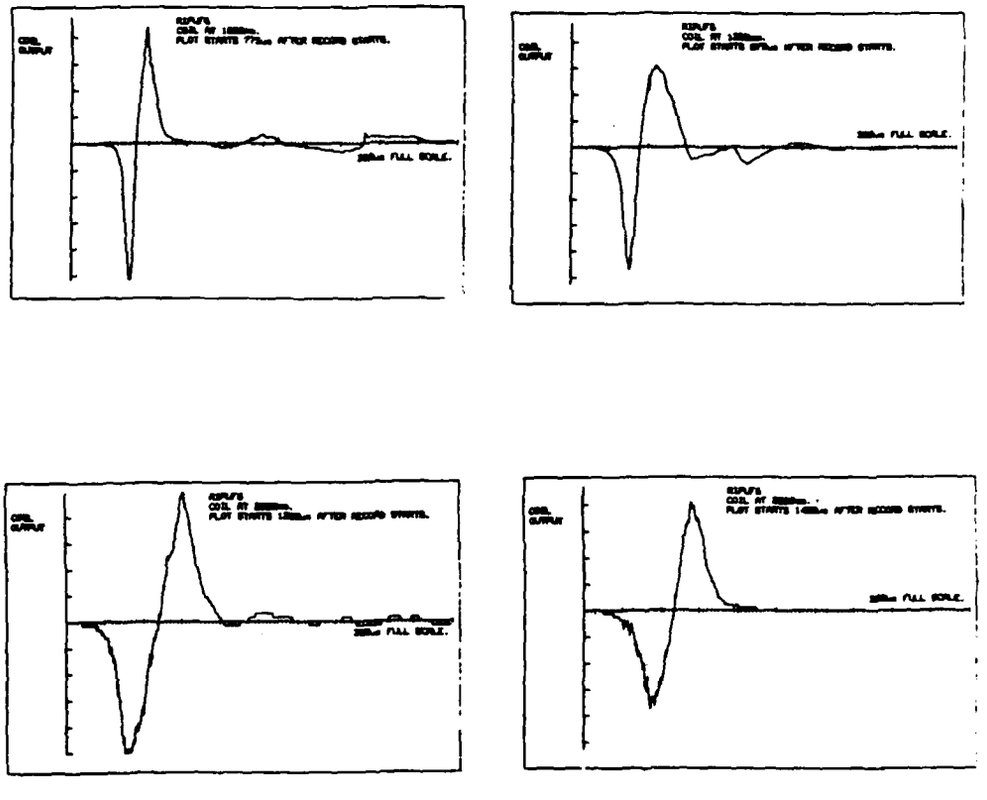

FIG. 43 Pick-up coil outputs - second puff-switched shot, continued

Interpretation of the pick-up coil waveforms requires care. The distance of the coils from the plasma should be as short as possible. At distances that are large compared to the bore dimensions all current distributions will give sinusoidal-type waveforms. The time between the peaks of each pick-up coil waveform can be used to obtain a rough estimate of plasma length, but the accuracy of the estimate depends greatly upon the distance of the coil from the plasma and to the current distribution in the plasma. To assist in the determinaton of current distribution and plasma length from pick-up coil waveforms, theoretical waveforms have been plotted for several current distributions [9]. Figure 44 gives some theoretical waveforms for the distance (7.5 mm) used in these experiments between the bottom of the bore and the centre of the pick-up coils.

Study of the calculated waveforms leads to the following four conclusions.

Firstly, if the plasma length is 5 to 10 times the bore dimensions, then uniform current distribution over the plasma length is distinguished by pick-up coil waveforms which have two odd-symmetrical peaks separated by an inflection or flat region. The flat region between the peaks increases in duration as plasma length increases. See Fig 44 (a).

Secondly, if the current distribution is not constant along the plasma length, but is symmetrical about the middle of the plasma length, the waveforms also have odd-function symmetry. See Fig 44 (b). There is no, however, inflection or flat portion between the peaks, and, for the longer plasmas, the peaks are distinctly rounded.

Thirdly, current distributions which are unsymmetrical about the centre of the plasma length produce waveforms with no symmetry. See Figs 44 (c) and 44 (d). The waveforms have a sharper peak over the region of greater current density and a wider peak over the region of lower current density. These features become more noticeable for longer plasmas.

Fourthly, the peaks of the waveforms correspond closely to the ends of the plasmas only for uniform current distributions and then only for plasmas that are at least as long as they are high. For plasmas that are shorter than their height, the peaks occur a considerable distance outside the plasma length. For non-uniform current distributions the peaks fall inside the length of the longer plasmas.

The theoretical waveforms in Fig 44 were calculated assuming constant plasma velocity. During the passage of long plasmas (100 mm) past the pick-up coils, the velocity may increase significantly. This will cause the trailing end peaks (right hand ends in Fig 44) to be sharper and of greater amplitude.

Inspection of the actual outputs (Figs 38-43) shows that they have no symmetry, except for the coils located at the breech and muzzle-ends. The first peaks (i.e. the left hand end peaks) are narrower and higher than the second peaks. In particular, there is no inflection or flat portion between the peaks. From the previous discussion, these waveforms indicate that the

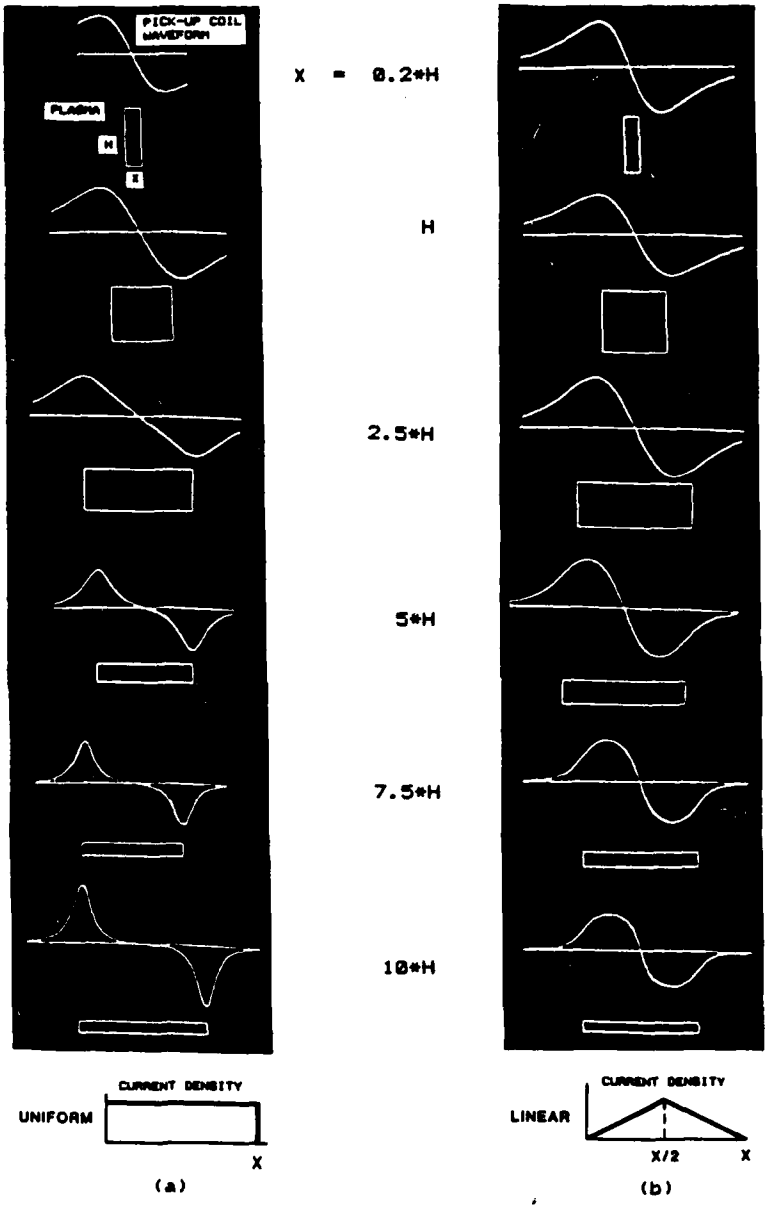

FIG. 44 Calculated pick-up coil waveforms at distance 0.75 H from the nearest plasma surface, for uniform and linear current distributions. The plasma is H x H in cross section and of length X and is shown beneath the waveforms.

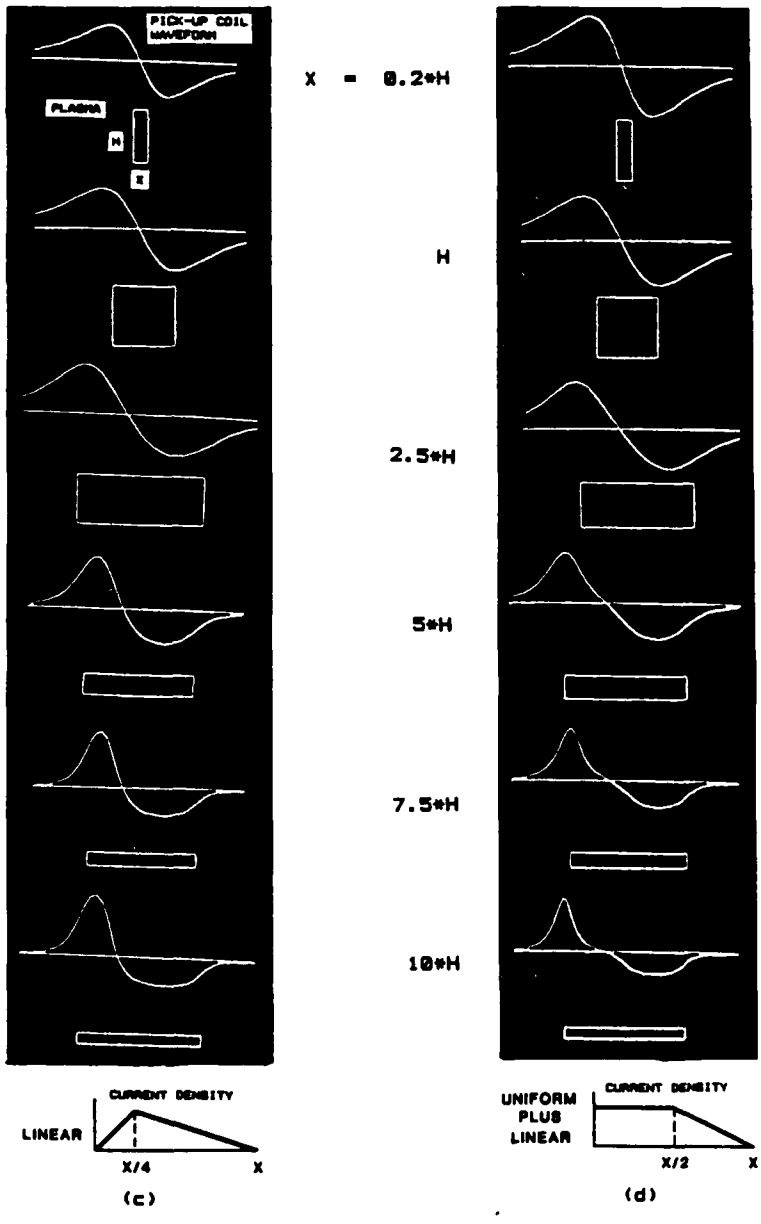

FIG. 44 (cont) Calculated pick-up coil waveforms at distance 0.75H from the plasma surface, for linear and uniform plus linear current distributions. The plasma is H x H in cross section and of length x and is shown beneath the waveforms.

current density rises rapidly to its peak value in the front part of the plasma and diminishes to zero over the rest of the plasma. Fig 44 (c) is a linear approximation to such a distribution. The absence of an inflection or flat region between the peaks indicates that the current is not uniformly distributed over any significant portion of the plasma length, i.e. it indicates that the current density is continuously changing along the plasma length.

The unsymmetrical waveforms obtained experimentally also indicate that the current spreads out from the rail-plasma interface to occupy much of the plasma. Rail damage frequently shows that current enters the plasma as arcs from the centre region of the rails; if these arcs passed directly from one rail to the other, like lightning strokes, the current would be concentrated in a thin sheet at the mid-plane of the plasma and would produce odd-symmetrical pick-up coil waveforms. Since only the current-carrying portions of the plasma are accelerated, such conduction between the rails would also imply that the plasma was thin at the front and increased to full bore height towards the rear as the "spent" plasma expanded.

Outputs with odd-symmetry were obtained only from the pick-up coil near the breech end (200 mm) or from the coils near the muzzle-end (2000 and 2250 mm). Because the plasma is short at the 200 mm position (the streak photographs indicate about 12 mm), any current distribution would give odd-symmetrical waveforms. No conclusion can, therefore, be drawn concerning the actual current distribution in the plasma.

The pick-up coil at 200 mm in the reference shot (Fig 38) shows that a period of zero voltage occurs between the peaks. The zero voltage region cannot be taken to indicate uniform current distribution because of the shortness of the plasma. This was the only such result in all the pick-up coil waveforms observed in railgun experiments at these Laboratories. The general reliability of the equipment and the experimental procedures was such that the zero voltage region is probably not an artifact. A possible explanation is that the current was carried in two separated regions, one at each end of the plasma with zero current in between. A computer simulation of such a double pulse using the technique set out in Ref. 9 yielded a waveform similar to Fig. 38, including the small oscillation in the region tween the peaks.

At the muzzle-end, the plasma is long (>100 mm) compared with the bore dimensions. The odd-symmetry of the waveforms from the muzzle-end coils can therefore be interpreted to mean that the current is concentrated about the centre of the plasma length and decreases symmetrically towards zero at each end of the plasma. As noted above, they may also indicate that the current is concentrated near the mid-plane of the plasma (i.e. the centre of the bore-height of the rails). The rail damage at the muzzle-end supports the interpretation that the current is concentrated near the centre of the plasma, both length-wise and height-wise (Section 3.2.6).

Many of the pick-up coil waveforms have minor peaks after the main peaks. The minor peaks indicate that current crossed from one rail to the other after the main arc had passed by. For example, the coil at the 1250 mm position in the Reference shot (Fig 39) indicates current flow 200-300 μs after the passage of the main arc. The waveform from the coil at 1500 mm has

much larger minor peaks, indicating that the plasma consisted of two main arcs. The streak photograph for this shot shows that at about 1500 mm there was a second arc which moved much more slowly.

Evidently the total current can sometimes pass through the plasma as a diffuse arc that is spread over the plasma length, and sometimes a small part of the current passes from one rail to the other at points that are well behind the main arc, and sometimes there are two main arcs, one of them lagging the other. A possible cause for the minor arcs is shorting of the rails by the soot that condenses from the trailing end of the plasma.

The coils at 800 and 1000 mm straddle the puff-switch region in the puff-switched shots. They show no significant variations from the pattern observed in the reference shot. Had a coil been placed at 900 mm it would be expected that to have shown the early strike of the arc between the puff-switch electrodes and later, the passage of the main arc.

The time between the positive and negative peaks, multiplied by the average velocity at the position of the pick-up coil, gives an estimate of the length of the current carrying portion of the plasma. From the earlier discussion it is evident that the estimate is accurate only when:

(i) the current is uniformly distributed over the length of the plasma;

(ii) the plasma is longer that it is high;

(iii) the pick-up coil is not more than the height of the plasma from the surface of the plasma;

(iv) the plasma velocity is constant while the plasma passes the pick-up coil;

Plasma lengths obtained in the reference shot by the pick-up coil method are given below, together with the lengths obtained from the streak photographs (Fig 20) for that shot.

Except at 200 mm, the lengths given by the pick-up coil method are less than the lengths measured on the streak photographs. These results support the conclusion that the current rises rapidly to a peak density near the leading edge of the plasma and tapers to zero over the remainder. Figure 44(c) shows that for such a distribution the peaks of the pick-up coil output lie within the plasma length, except when the plasma length is less than the plasma height. (The length obtained from the streak photograph at 1500 mm, viz. 374 mm, is excessive. This is because of the over exposure referred to in Section 3.3.1).

Comparison of plasma lengths from pick-up coil waveforms and from streak photographs

Position mm	Time between peaks μs	Plasma velocity km/s	Plasma length, pick-up coil method mm	Plasma length streak photograph (Fig 20) mm
200	31	1.2	37	12
400	24	1.76	42	46
600	25	1.85	46	60
80	29	1.89	55	70
1000	30	1.94	58	81
1250	29	2.0	58	81
1500	24	2.06	49	374
2000	35	1.3	46	127
2250	43	0.65	28	38

The length obtained from the 200 mm position coil, 37 mm, is about 3 times that measured on the streak photograph. As explained earlier, plasmas which are short compared to their height yield pick-up coil peaks that are outside the plasma length.

The calculated outputs show that the zero crossovers of the pick-up coil outputs correspond to the region of maximum current density. If the current were symmetrically distributed over the plasma length, the zero crossovers would occur in the centre of the plasma length and the pick-up coil outputs would have odd-symmetry. Except towards the end of the gun, the coil outputs in fact show that the zero crossovers are closer to the leading edges of the waveforms. These practical results imply that, whilst the plasma is accelerating, the current density is greatest near the leading edge of the plasma, and further support the previous conclusion that most of the current is near the leading edge.

The zero crossover points and the plasma leading edge data are plotted in Figs. 45 and 46 for the reference and puff-switched shots. Where the leading edge is accelerating, the zero crossover points lie within 20 mm of the leading edge. In the reference shot the zero crossover falls back to 60-70 mm from the leading edge at the 1500 and 2000 mm distances. The last zero crossover, at 2250 mm, apparently moves back towards the leading edge but this effect is due to the plasma length being only 30 mm at this point. The crossover in fact is near the centre of the plasma.

Due to increasing plasma length and decreasing current, the average current density in the plasma decreases with distance from the breech. This observation and the above results suggest that so long as average current density is high enough, Lorentz forces can move electrons towards the leading edge and maintain the edge in a state of relatively high conductivity, e.g. by

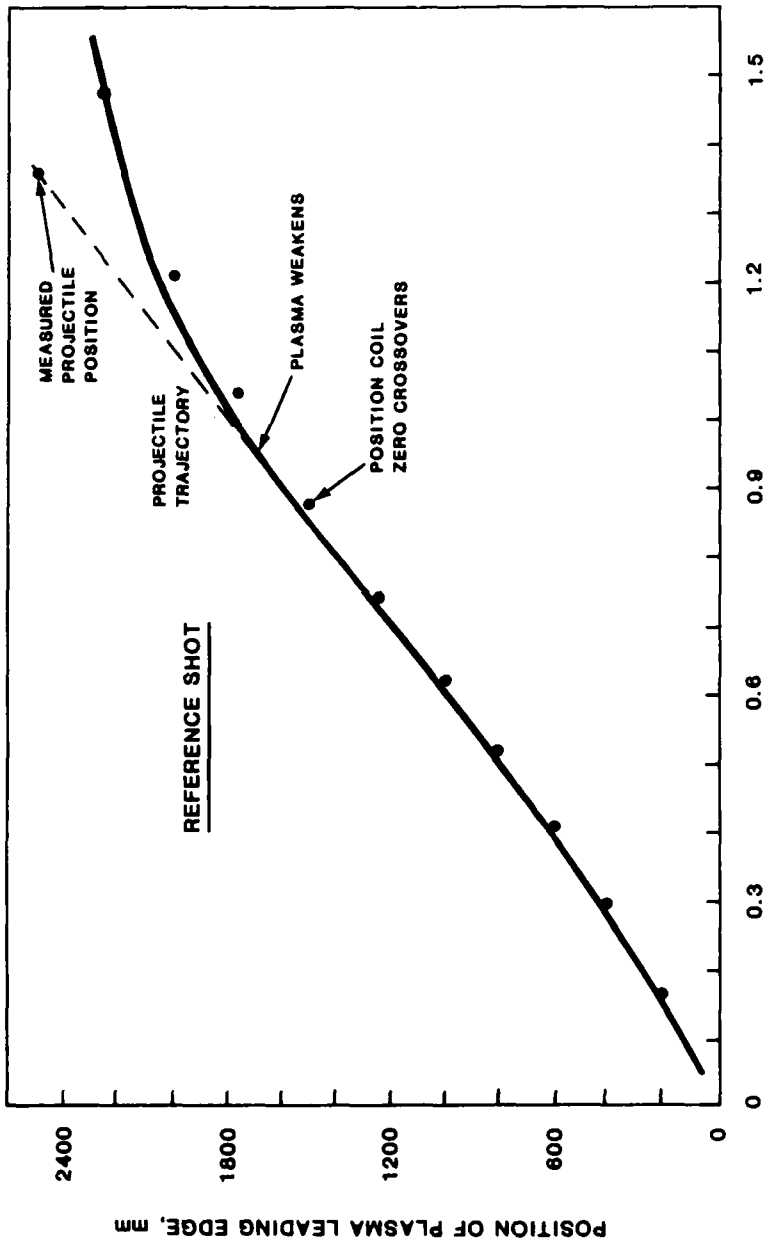

FIG. 45 Plasma leading edge and zero crossovers of pick-up coils

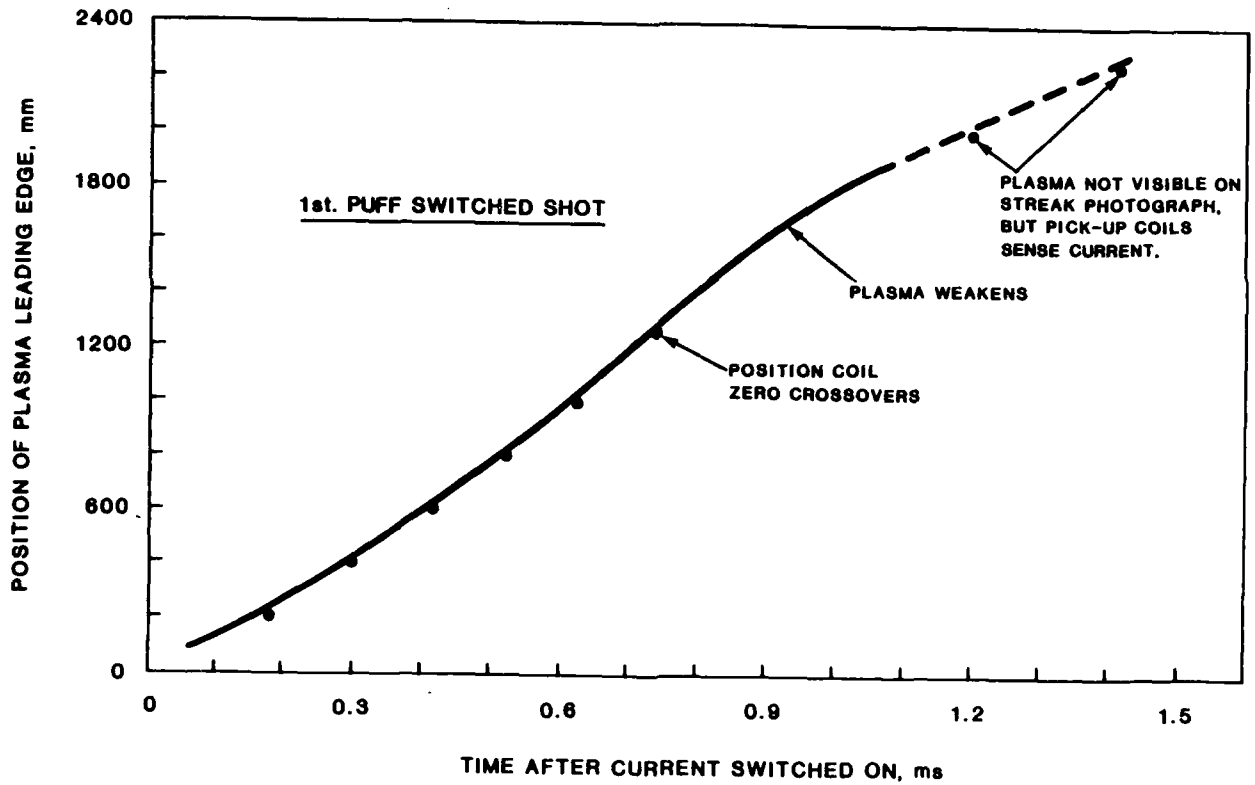

FIG. 46 Plasma leading edge and zero crossovers of pick-up coils

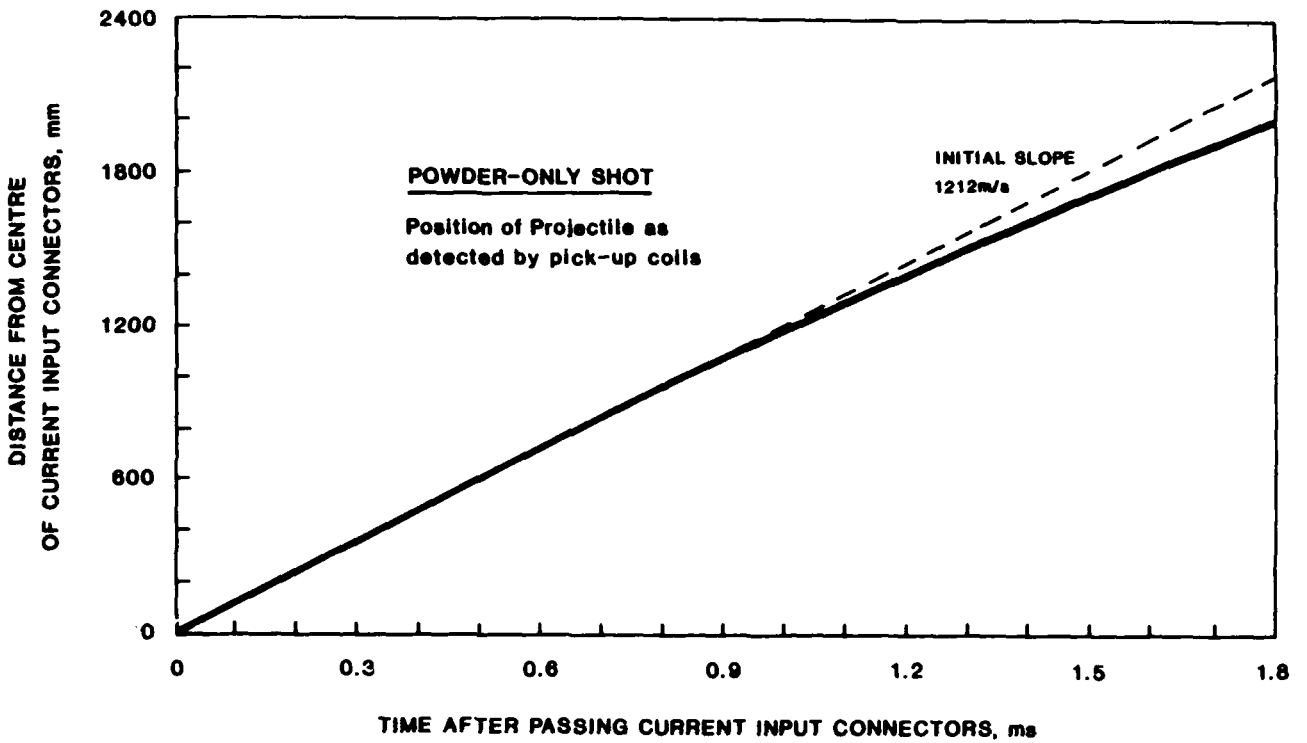

FIG. 47 Position of projectile in powder-only shot as detected by pick-up coils

cumulative breakdown. When the average current density falls, the Lorentz forces are dissipated in more complex collision paths and conductivity is greatest near the centre of the plasma length, where it is hotter, resulting in a more symmetrical current distribution over the plasma length.

The pick-up coil crossover points for the powder-only shot are plotted in Fig. 47. For about a third of the length of the gun there is practically no departure from a straight line, indicating that friction was very low. As Fig. 25 shows more clearly, the velocity dropped further along the barrel. From the injection and exit velocities it can be calculated that the average opposing force was about 330 N. The force needed to push the projectile by hand was much less than this. Deformation of the projectile may have caused increased friction, but, since the barrel was not evacuated, compression of air ahead of the projectile may also account for the large opposition force.

3.2.5 Source of Propulsive Energy

The intention in the railgun is to propel the projectile by Lorentz, or $q\,\underset{\sim}{v} \times \underset{\sim}{B}$, forces that act upon the electrons as they cross the magnetic field between the rails. In the above formula q is the electron charge, $\underset{\sim}{v}$ is the electron velocity and $\underset{\sim}{B}$ is the magnetic field intensity due to the current in the rails. The plasma, however, in addition to providing electrons which are acted upon by Lorentz forces, is an electrically heated gas and a question of interest is to what extent the projectile is pushed by gas pressure that arises directly from the explosive-like effects of the rapid electrical heating.

The velocity-time and current-time records enable this question to be investigated. The current record of the reference shot Fig. 26, shows that the breech-supplied current rose sinusoidally from zero to a peak value of 116 kA in 250 μs. Inspection of the velocity record, Fig. 24, suggests that the plasma (and hence projectile) acceleration was not in phase with the acceleration to be expected from the current waveform. There was little increase in velocity for about 150 μs, by which time the current had reached 95 kA, or 82% of its peak value. The velocity also continued to increase rapidly for 50 μs after the current had begun to decline and then, without any significant fall in current, its rate of increase suddenly dropped.

The inference from the above observations is that the velocity was strongly affected by another factor. Calculation of the velocity and energy increments that could have accrued from the Lorentz forces supports this inference. If the ideal railgun force, viz:

$$F = \frac{1}{2} L' I^2$$

where L' is the high frequency inductance of the rails per unit length and I is the current, were the only factor then the velocity increase, Δv, during the quarter cycle of sinusoidal current rise to peak value I_p, would be:

$$\Delta v = \frac{L' I_p^{\,2} T_{1/4}}{4M}$$

where $T_{1/4}$ is the quarter-cycle time. Substituting values for this case, viz:

$$L' = 0.407\ \mu H/m$$

$$I_p = 116\ kA$$

$$T_{1/4} = 250\ \mu s$$

$$M = 1.2 \times 10^{-3}\ kg$$

yields $\Delta v = 290$ m/s. From Fig. 24 it is found that the velocity actually increased from 1155 m/s to 1600 m/s, i.e. by 445 m/s in the 250 μs period, which is about 1.6 times the maximum increase that the Lorentz forces could have caused. Extending the calculation to cover the next 50 μs shows that Lorentz forces could have increased the velocity by a further 110 m/s whereas in fact the velocity increased by about 150 m/s.

It is therefore clear that additional forces were present in the first 300 μs. The most obvious source is the impact of high velocity particles during the explosive-like formation of the plasma. Inspection of the streak record for the reference shot shows that prior to 400 mm, which corresponds to 300 μs, the plasma had not fully formed. Rapid acceleration occurred while the foil vapour and other matter from the bore surfaces was expanding from a superheated, dense fluid state to an equilibrium condition characterised by more or less constant plasma length.

After 300 μs the thrust from the explosion ceases and for the next 500 μs the velocity increases at a much lower rate. In this region the principal cause of acceleration should be the Lorentz forces. Figure 26 shows that the current diminished in a linear fashion from 113 kA at the rate of 94×10^6 A/s in the period from 300 μs to 800 μs after the commencement of conduction. Writing the current during this period as

$$I = I_o - kt$$

where I_o is the initial current (103 kA) and $k = 94 \times 10^6$ A/s and substituting in the basic force expression and integrating yields the velocity increase, Δv, to be:

$$\Delta v = \frac{L't}{2M} \left[I_o^2 - kI_o t + \frac{k^2}{3} t^2 \right] .$$

Substituting $t = 500\ \mu s$, and the other values as previously given, yields $\Delta v = 552$ m/s.

From Fig. 24 it is found that the actual velocity increase of the reference shot from 300 μs to 800 μs was 300 m/s. On the assumption that friction and the explosive effects were negligible, this result enables an effective inductance gradient, L'_{eff}, to be calculated as

$$L'_{eff} = \frac{300}{552}(0.407) = 0.22\ \mu H/m,$$

or about half of the high frequency value. As it is likely that there was still some explosive drive, this is probably a high estimate.

Using the above L'_{eff} value, the velocity increase due to Lorentz forces during the first 300 μs is found to be 206 m/s compared to the actual increase of 595 m/s, and hence the explosive effect contributed 389 m/s.

The energy which the Lorentz forces would then have supplied during the first 300 μs is 311 J out of an actual gain of 1037 J. For the whole period to 800 μs the energy increment was 1741 J of which 1015 J can be attributed to acceleration with L'_{eff} = 0.22 μH/m and the remaining 726 J, or about 42% of the total, to the explosive formation of the plasma.

The increase of velocity following the injection of the puff-switched current in the first puff-switched shot is similar in shape to the initial increase and is also similarly displaced from the current waveform (Figs. 24, 28), which implies that the explosion-like formation of the arc between the puff-holes was responsible for most of the velocity boost.

3.2.6 Rail Damage

The length of this gun and the range of current densities in the plasma resulted in a greater variety of arc damage to the rails than that in the shorter guns (< 1 m) generally used at these Laboratories.

Five broad types of rail damage were noted, and are shown in Fig. 48. They are, in order of appearance from the breech end:

(a) Sand blasted effect. This type of damage starts in a patchy manner at the breech end where the foil explodes and can cover the whole exposed rail width.

(b) Broad parallel streaks with diverging feathery edges. There are two to five such streaks. The pattern covers the bore width of the rails and the diverging feathery pattern is concentrated along the outer edges.

(c) Finer, more or less parallel streaks. Typically there are two to five streaks, 10-30 mm long, which are confined to the central half of the rails. Sometimes the streaks are confined to a narrow channel in the centre of the rails.

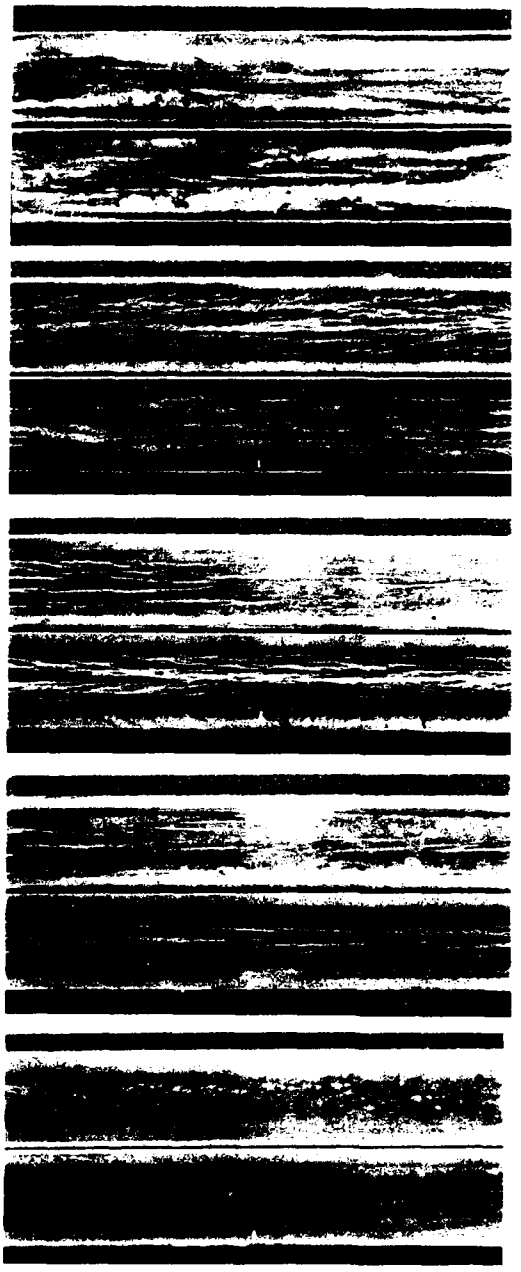

(a) 117 mm from breech end
Gross damage, sand-blast effect.

(b) 626 mm from breech end
Broad parallel streaks with diverging feathery edges.

(c) 985 mm from breech end
Finer, more or less parallel streaks

(d) 1320 mm from breech end
Converging, fine streaks

(e) 2305 mm from breech end
chains of deep pits

FIG. 48 Types of rail damage - reference shot Upper rail is negative, breech end is left hand end.

(d) Converging streaks. Typically there are two to five main streaks, 10-30 mm long, converging at 10-15^{o} to the rail length. They are confined to the central half of the rail width.

(e) Chains of deep pits. Typically there are two chains and each is about 30 mm long and they are confined to the central half of the rail width.

The photographs in Fig. 48 are from the reference-shot rails. Similar damage patterns were produced on the rails in the puff-switch shots.

Patterns (c) to (e) have an additional fine structure which has the appearance of tangled fine scratches (as if made by steel wool) that converge from the outer edges towards the centre. In (e), this pattern also becomes arc-pitted, although the pits are small.

When examined through a magnifying glass the streaks, other than the broader streaks emanating from the "sand blast" affected areas, are seen to consist of numerous small furrows and pits.

The "sand-blasted" areas and broader streaks appear under the magnifying glass to be a surface layer of melted metal upon relatively cold bulk metal. They also appear to have been smeared in the direction of motion of the plasma.

The above progression of damage patterns is explicable in terms of diminishing thermal energy density and diminishing regions of conductivity in the plasma, as follows.

For the first 200 mm of travel the plasma is short (the streak photographs indicate about 10 mm at 200 mm). The energy density in the plasma, and consequently the plasma temperature, is high compared with conditions when the plasma has expanded. During this early phase, atoms and ions bombard both the rail surfaces due to the high pressure of the plasma. The bombardment melts and vapourizes the surfaces and also deposits metal that was vapourized earlier. Because of the injection velocity of about 1 km/s the contact between the developing plasma cloud and the rails may be patchy. The above interaction of the plasma and the rails results in the "sand-blasted" and "smeared" appearance. (The "smeared" appearance has previously been described as "wind-swept" [10]). Evidence for this bombardment model has also been seen in firings using aluminium foils, where the "sand-blast" areas have a distinct golden colour, suggesting alloying with aluminium [9]. To form such an alloy, aluminium atoms must have been ejected from the plasma into a molten layer of copper.

The streaks composed of furrows and pits that appear later are not present in the "sand-blast" affected areas. This suggests that the entire area in contact with the plasma was conducting in a diffuse manner. Diffuse conduction at the surface is known to occur in arcs upon materials such as tungsten and carbon. The vapourization temperatures of these materials are above the temperatures necessary for copious thermionic and field emission of electrons [11]. Such emission is not normally produced by copper because of its low vapourization temperature (2,800K). However, if the temperature of

the copper reaches about 6,000 K due to the hot high power arc in the railgun (i.e. it is superheated), sufficient thermionic emission would occur.

The length of the plasma increases due to expansion as a hot gas and also due to material vapourized from the four sides of the bore. Because of the expansion, cooler zones arise in the plasma. The current divides into the hottest regions, because they have the greatest conductivity. These current-carrying hot regions are driven by Lorentz forces and produce the broad streaks of "sand-blast" surface that emanate from the earlier "sand-blast"damage.

Further expansion of the plasma results in temperatures in the surface regions of the plasma that are too low to melt the rail surfaces and too low to cause substantial thermionic emission. "Cold" arc processes then take over with the production of anode and cathode spots [12]. The Lorentz forces drive the individual arcs along the rails and cause parallel tracks, consisting of overlapping furrows and pits, to be left in the rail surface. The arcs are imagined to be confined to the cool outer layers of the plasma; within the hot body of the plasma the current is diffuse. This model is discussed in more detail in Ref. 9.

The streak patterns that are nearly parallel suggest that conditions were suitable for arcs to be driven by Lorentz forces as desired for railgun propulsion. One necessary condition is that the current near the plasma leading edge must produce free electrons at a sufficient rate to support current flow in the region ahead. As was mentioned in Section 3.2.4 this requires current density in the plasma to be sufficiently high.

The diverging feathery pattern that sometimes appears on the outer edges of the broad streaks may be due to inadequate sealing. In the reference shot it appeared at the breech end and in the first puff-switched shot it appeared at both the breech end and after the puff-switch section. In the second puff-switched shot it did not appear at the breech end, where the sealing had been improved, but it did appear after the puff-switch section, where it is known that the halves of the body separated. This explanation is consistent with the disappearance of the diverging feathery pattern at the same distances as those at which the rapid velocity boosts finished.

The next broadly discernible pattern, viz. fine streaks which converge towards the centre of the rails at angles of $10\text{-}15^{\circ}$, may be due to the outer bulk of the plasma becoming cool and causing the arc paths to converge to the centre, which is hottest and most conductive. The angles suggest that the arcs move towards the centre at about a quarter of the plasma velocity.

The deep arc craters that appear near the muzzle end are consistent with continuing fall of plasma temperature and the contraction of the conductive regions to the centre. Electrons propelled by Lorentz forces

cannot produce sufficient secondary electrons in the colder regions and the current is confined to a particular conductive channel for a longer period.

Both rails of the guns exhibited the same general type of damage at the same distance, but often differed in detail. For example, at one position on the reference-shot rails, one rail has five or six short converging tracks but the opposite rail has two or three longer tracks.

3.2.7 Ablation model – puff-hole venting

Parker et al [13] have proposed that increasing plasma mass, due to ablation of wall materials at the high temperatures of the plasma, causes the plasma to reach a limiting velocity, v_L, given by

$$v_L = \frac{L' I_o}{2\alpha V_a},$$

where L' is the inductance per unit length, I_o is the (constant) current, α is the ablation constant and V_a is the arc voltage. A characteristic time, τ, is also defined by

$$\tau = \frac{M_p}{\alpha I_o V_a},$$

where M_p is the mass of the projectile. The actual velocity attained in time t is then given by

$$v = v_L \frac{t}{t + \tau}.$$

This theory, and particularly its extension to include drag due to turbulence adjacent to bore surfaces, also given by Parker et al, predicts such low velocities as to make the plasma arc method of propulsion unpromising. It is therefore important to compare results with this theory.

A criticism of the theory is that it assumes that all the plasma mass is accelerated. The fact that bore surfaces are completely covered with black soot containing carbon and copper [14] suggests that material is continually deposited from the plasma. Such deposition is supported by streak photographs with longer exposures (e.g. the muzzle end streak of the reference shot, Fig. 20) which show stationary hot material for about 100 μs after the moving part of the plasma has passed by. The concentration of current at the plasma leading edge also suggests that material at the rear is left behind and deposited.

Parker et al proposed that allowing some plasma to escape through vents is one way to reduce its mass. The reference shot, which included 2 mm diameter puff-holes, provided a convenient test of this idea.

When the reference shot was fired a large shower of flame and red sparks erupted from the vents, as from a firework. From this it could be expected that the streak record would show the plasma to be shortened in length or weakened in intensity. Fig. 20 however shows virtually no effect. Likewise, there was barely any effect on the muzzle voltage or on the slope of the velocity curve (Figs. 36, 25). An explanation could be that the puff-holes were too small, despite the eruption observed, but the result also could imply that plasma regeneration is rapid. This latter conclusion was reached
in earlier puff-hole experiments where larger holes were used [7].

Despite the objections which may be raised, the expressions above give velocities that are comparable with those measured if a suitable "average" value of current is selected. It is necessary to select such a value since current is not constant. Thus, using the preceding equations with the values

L' = 0.407 μH/m,

α = 25 g/MJ, as suggested by Parker et al.

I_o = 70 kA, "effective" value, Fig. 26

V_a = 190 V, average value, Fig. 36

yields the limiting velocity, v_L, as 3000 m/s and the characteristic time, τ, as 3.6 ms. Figure 24 shows that the maximum velocity was reached after 0.8 ms. According to the expressions above, the velocity increment in this time would be 545 m/s. The actual increase was 903 m/s (1155 m/s to 2058 m/s) which leaves 358 m/s to be attributed to the explosion of the foil. This latter value is in fair agreement with the foil explosion contribution of 389 m/s deduced in Section 3.2.5. The inclusion of drag as proposed in the extended ablation model would lower the calculated velocity increase and bring the increase due to the foil explosion into better agreement.

Because the agreement with the ablation model is quite sensitive to the "effective" current value no firm conclusion can be made as to its validity.

3.2.8 Data Tabulation

Distances were measured from the centre line of the current input electrodes, where they were connected to the rails.

Times were measured from the time at which the breech current supply commenced, i.e. the time at which current commenced to rise after the ignitron was triggered. A 10 μs marker pulse was coupled into most transient recorders simultaneously with the ignitron trigger pulse. The time zero is

slightly different from the time at which the projectile passed the centre of the current input electrodes. The intention was that current should not be switched on until the projectile was 10-20 mm past this point.

Great care was taken to ensure that two or three independent records were obtained to determine the zero reference for time measurement. The times given are accurate to within ± 3 μs.

Pick-up coil arrival times (microseconds)

Position (mm)	Powder-only	Reference	1st Puff-Switch	2nd Puff-Switch
200	163	167	172	204
400	328	295	303	344
600	494	407	414	460
800	667	519	523	563
1000	839	617	622	669
1250	-	741	737	775
1500	1299	870	-	-
1750	-	1037	-	-
2000	1799	1204	1192	1169
2250	-	1475	1404	1368

Arrival times are zero crossover times for the electrical shots and the times to the centres of the pick-up coil waveforms in the case of the powder-only shot.

Transient recorders failed to trigger in some cases. The values are left blank in the table. Time zero for the powder-only shot is when the projectile passes the centre of the current input electrodes.

Time of arrival of plasma leading edge using streak records (microseconds)

Position (mm)	Reference	1st Puff-Switch
100	63	57
200	149	156
300	226	231
400	281	293
500	339	339
600	395	406
700	449	457
800	500	509
900	554	562
1000	604	613
1100	653	659
1200	709	705
1300	754	752
1400	801	795
1500	850	838
1600	901	885
1675	939	-
1700	-	938
1725	968	-
1800	1024	1004
1900	1102	1073
2000	1172	-
2100	1259	-
2200	1381	-
2300	1537	-

Velocity of plasma leading edge using streak records (± 2%)

Position (mm)	Velocities (m/s) Reference	1st Puff-Switch	2nd Puff-Switch
Injection	1155	1155	1000
200	1214	-	
300	1512	1416	
400	1755	1737	
500	1755	1763	
600	1854	1864	
700	1854	1864	
800	1878	1902	1816
875	-	-	1678
900	1903	1902	-
925	-	-	1755
1000	1940	1927	5208
1100	1940	2158	1986
1200	1940	2183	2315
1300	2003	2248	2359
1400	2058	2248	2462
1500	2058	2186	2462
1675	2003	-	-
1700	1300	1802	1897
1800	1300	-	-
1900	1300	1023	1630
2000	1300		1256
2100	1300		1256
2200	645		1132
2300	645		1132
Exit	1923	2100	2315

(measured over 500 mm flight in air from muzzle to break-screen)

3.3 Cause of Early Switching

Possible causes of the early triggering of the puff-switched supplies can be grouped into two classes: action-at-a-distance effects, which the intense electromagnetic and optical radiation might cause, or the direct introduction of conducting matter into the space between the rails and the puff-switch electrodes.

Action-at-a-distance effects were shown to be unlikely by a subsequent test. In this test the puff-switched capacitor bank was charged to 4.5 kV and the ends of its busbars were exposed to the muzzle flash of a short railgun. The busbar ends were angled to a separation of about 20 mm where they connect to the puff-switch (which was not connected during this test) and were shielded from physical contact with the flash by a perspex cover. The separation between the railgun muzzle and the busbar ends was about 200 mm. The bank did not discharge when the railgun was fired.

The above test suggests that early triggering was due to the introduction of conducting matter into the puff-switch region. One possible cause might be that ionized air was pushed ahead of the projectile. This possibility was discounted because the rails would discharge the ions. The fact that the much smaller puff-holes in the second firing were ineffective suggests that early triggering would have occurred even if there had been no puff-holes. This in turn leads to the possibility that arc pressure may have separated the halves of the gun body sufficiently for plasma to escape over the edges and along the backs of the rails into the puff-switch region, despite the sealing in the second firing.

Examination of the halves of the railgun body clearly showed that it separated after the puff-switch operated; an area extending about 100 mm either side of the puff-switch electrodes was blackened with the fine soot (Fig. 17) and, further along the body, black soot was deposited between the bolt holes. In the first puff-switched shot, and in the reference shot, fine black soot covered the edges of the rails and about half of the back of the rails, virtually from the breech to the muzzle. In the second shot the sealant in the rail channels of the body and on the edges of the rails was found to be wstreaked with black soot in a number of places between the breech and where triggering occurred. The backs of the rails were also covered with soot for about 100 mm on the breech side of the puff-switch electrodes.

Calculation of the tension in the bolts used to hold the halves of the body together shows that the bolts almost certainly yielded during tightening. The bolts, 12 mm diameter with coarse thread and medium tensile strength, were tightened with an air wrench to about 80 Nm torque, which implies a tensile stress of about 400 MPa, or 60,000 lbs/sq in. This is well into the yield region of steel. The additional tension in the bolts due to the passage of the plasma may be inferred from the acceleration of the 1.2 g projectile and the plasma length. Thus, the projectile velocity increased by 600 m/s in 300 μs after injection, implying a plasma pressure of 24 MPa. The force on the halves of the gun body over the 70 mm plasma length was therefore 16.8 kN and, if shared by 4 bolts, yields an increase of about 54 MPa

(8,000 lb/sq in) in bolt tensile stress. The peak tensile stress in the bolts prior to the puff-switch operation was therefore about 450 MPa.

4. SUMMARY AND CONCLUSIONS

The sequence of experiments enabled the following aspects of railgun technology to be investigated:

(i) a simple means of connecting additional power sources, viz. puff-switching;

(ii) distribution of current in the plasma;

(iii) energy distribution, in particular the sources of the projectile kinetic energy;

(iv) types of rail damage in relation to current density in the plasma;

(v) velocity limitation according to the ablation model.

Streak photography through a clear body was a most important diagnostic means, particularly when correlated with accurate distance and time calibrations and with pick-up coil and voltage and current data. These records enabled times from a common reference instant to be known to within a few microseconds and distances from a common reference point to be known to within a few millimetres.

The five aspects identified above are summarized in greater detail below.

Puff-switching: The experiments demonstrated that a second power source can be connected by a puff-switch. The implementation of the idea in these experiments was not successful, but high sensitivity switching which the method displayed suggests that a satisfactory design is possible. Such a design might be along the lines indicated in Fig. 49. In this design there is one puff-hole in the bore between the rails and the plasma triggers an arc gap in one of the busbars from the second power source. The puff-hole is not in the current path and hence the switching arc, being outside the gun, is not able to form a stationary arc from one rail to the other. The time delay in switching can be adjusted by the distance to the spark gap switch to ensure that early triggering does not cause significant reverse current flow. Also, there is only one arc drop compared with two in the configuration tested (Fig. 2) and therefore the rate of fall of puff-switched current is reduced, so the current is effective for a longer time. Sealing of the gun bore is not so critical and the electrodes can be much stronger and better able to withstand the arc pressures than those in the trial design of these experiments.

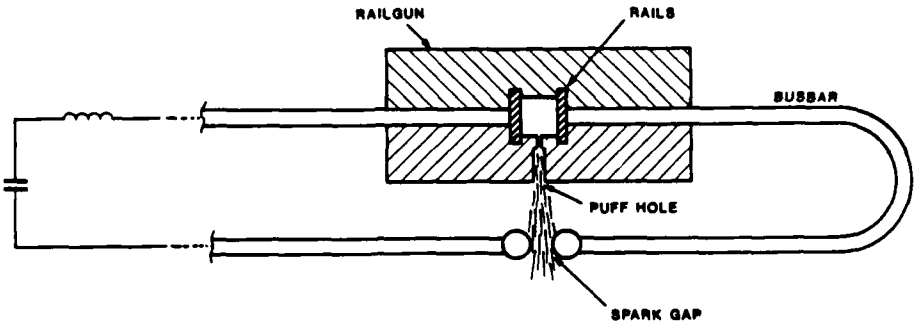

FIG. 49 Improved puff-switching implementation

Distribution of current within the plasma: The shape of the outputs from the pick-up coils and the location of the zero crossovers, in conjunction with the streak photographs, showed that the current is concentrated within about 20 mm of the leading edge of the plasma and tapers off towards the rear end, in those periods when the plasma is accelerating strongly. When the plasma is weak, the current is symmetrically distributed along the plasma length. Sometimes small portions of the current flow from one rail to the other long after the main current has passed (e.g. 100 μs); this may be due to conduction via condensed soot on the polycarbonate surfaces.

Energy distribution: About 30 kJ of the 72 kJ stored on the breech supply capacitors was lost during transfer to the storage inductor. This loss is typical and suggests that more efficient methods of charging the inductor should be investigated. About 2.4% of the electrical energy stored on the capacitors became projectile kinetic energy in each instance. At least 40% of the projectile kinetic energy gain was probably due to the explosive formation of the plasma arc, both at the breech and puff-switched connections. The effective inductance gradient was about 0.22 μH/m, compared with the theoretical value of 0.407 μH/m.

Rail damage: The length of the railgun and the variation of current values enabled a sequence of five types of rail damage to be identified, viz.

melted surfaces (sandblasted appearance);
broad parallel streaks;
fine parallel streaks;
converging streaks;
chains of arc pits.

The above progression was explained in terms of the decreasing current density of the plasma from the breech towards the muzzle, owing to decreasing current and increasing plasma length. Streaks converge towards the centre, where the plasma is hottest and most conductive. The diverging feathery edges were thought to be due to plasma escaping past the rails because of inadequate sealing.

Ablation model: This model seems to ignore the evidence that material is deposited from the plasma and therefore not all ablated material increases the accelerated plasma mass. However, the predictions of the model with a not unreasonable choice of values for the variables do fit the results obtained. A definite statement in favour of the model cannot be made on the basis of these limited investigations.

A final conclusion concerns the gun length and the magnitude of current for experimental railguns. To study the intended electromagnetic propulsion, the explosive drive during the plasma formation must have ceased but the plasma must not be failing. Since the explosive drive lasts about 300 μs, railguns that use injection at about 1 km/s should be at least 1 m long. The current must be kept high enough for as long as possible after the explosive drive ceases so that electromagnetic drive does not cease owing to failure of the plasma.

5. ACKNOWLEDGEMENTS

This work was carried out with the support of the US Defense Advanced Research Projects Agency (DARPA).

Dr R.A. Marshall was the driving force behind the puff-switching concept. Although he left MRL in the early stages of this work his availability for discussion and comment has been much appreciated.

Mr G.A. Clark took part in many aspects of the work and if it were not for other commitments would have been a co-author.

Mr W.A. Jenkins assisted in the developmental and experimental aspects of the whole electromagnetic launcher program at these Laboratories and his contributions are gratefully acknowledged. He also suggested the improved puff-switch configuration described in Section 4.

Mr J. Ferrett provided much valuable assistance in the construction and installation aspects and during firings and in the subsequent preparation of graphical and photographic data.

Finally, the authors wish to thank Dr C.I. Sach, Head of Electrodynamics Group, for his encouragement and his constructive criticism in the preparation of this Report.

6. REFERENCES

1. Marshall, R.A. (1979). Railgun Overview. Proceedings of the Impact Fusion Workshop, Los Alamos Scientific Laboratory, Los Alamos, New Mexico, LA8000C, 128-145. (Compiled by A.T. Peaslee).

2. Marshall, R.A. and Weldon, W.F. (1980) Analysis of Performance of Railgun Accelerators Powered by Distributed Energy Stores. Proceedings of the 14th IEEE Pulse Power Modulator Symposium, Orlando, Florida, 318-322.

3. Parker, J.V. (1982). Electromagnetic Projectile Acceleration Utilizing Distributed Energy Sources. J. Appl. Phys., Vol 53, No 10, 6710-6723.

4. Holland, L.D. (1984). Distributed-Current-Feed and Distributed-Energy-Store Railguns. IEEE Trans. on Magnetics, Vol MAG-20, No 2, 272-275.

5. Holland, L.D. (1984). The DES Railgun Facility at CEM-UT. IEEE Trans. on Magnetics, Vol MAG-20, No 2, 256-259.

6. Tower, M.M. and Haight, C.H. (1984). Development of a High-energy Distributed Energy Source Electromagnetic Railgun with Improved Energy Conversion Efficiency. IEEE Trans. on Magnetics, Vol MAG-20, No 2, 298-301.

7. Marshall, R.A. (1984). Plasma Puffing from a Railgun Armature. IEEE Trans. on Magnetics, Vol MAG-20, No 2, 264-267.

8. Clark, G.A. and Thio, Y.C. (1984). Design and Operation of a Self Activating Crowbar Switch. IEEE Trans. on Magnetics, Vol. MAG-20, No 2, 364, 365.

9. Stainsby, D.F. and D.R. Sadedin. Experiments with a Small Injected Railgun. MRL Report MRL-R-1055.

10. Bedford, A.J. (1984). Rail Damage in a Small Calibre Railgun. IEEE Trans. on Magnetics, Vol. MAG-20, No 2, 348-351.

11. Martin, T.L. (1957). Physical Basis for Electrical Engineering. Prentice Hall, Inc., Englewood Cliffs, N.J. 1957, pp 303.

12. Lafferty, J.M. (Ed). (1980). Vacuum Arcs Theory and Application. John Wiley and Sons pp 4, 5.

13. Parker, J.V., Parsons, W.M., Cummings, C.E. and Fox, W.E. (1985). Performance Loss Due to Wall Ablation in Plasma Armature Railguns. AIAA 18th Fluid Dynamics and Plasmadynamics and Lasers Conference.

14. Bedford, A.J. (Materials Research Laboratories) (1986). Personal communication.

15. Macintyre, I.B. (1985). High speed photographic analysis of railgun plasmas. Proceedings, 16th International Congress on High Speed Photography and Photonics, Aug 27-31, 1984, Strasbourg, France, pp 938-945 (Society of Photo-Optical Instrumentation Engineers, Washington).

END

DATE
FILMED

588